Chemical Engineering Journal 498 (2024) 154920

Contents lists available at ScienceDirect

Chemical Engineering Journal

journal homepage: www.elsevier.com/locate/cej

Review

Advanced cold plasma-assisted technology for green and sustainable ammonia synthesis

Deepak Panchal [a], Qiuyun Lu [a], Ken Sakaushi [b], Xuehua Zhang [a,c,*]

[a] Department of Chemical and Materials Engineering, University of Alberta, 9211 116 Street, NW, Edmonton, Alberta, T6G 1H9, Canada
[b] Research Center for Energy and Environmental Materials, National Institute for Materials Science, 1-1 Namiki, Tsukuba, Ibaraki, 305-0044, Japan
[c] Physics of Fluids group, Faculty of Science and Technology, University of Twente, P.O. Box 217, Enschede, 7500 AE, Netherlands

ARTICLE INFO

Keywords:
Plasma
Ammonia
Catalysis
Energy
Sustainable

ABSTRACT

Ammonia (NH_3) is the most crucial industrial chemical feedstock for producing fertilizers and is a promising future hydrogen carrier. Recent research has spurred for the development of alternative green and sustainable ammonia production technologies. Cold plasma technology provides a clean, sustainable method for nitrogen (N_2) conversion into active species for ammonia synthesis. Synergistic action of cold plasma and catalyst has significantly improved the current production rate and selectivity. Present energy consumption (2.1 MJ mol N^{-1}) for N_2 fixation via plasma-assisted technology is still higher than the commercial process (0.7 MJ mol N^{-1}), while a further improvement would be game-changing. In this review, we explain the takeover by plasma-assisted technology and its potential for green and sustainable ammonia production. We briefly present that the major challenge in nitrogen fixation of N_2 to NO_x as an intermediate pathway, can be addressed by plasma technology via NO_x transformation into targeted NH_3 product. We discussed the emerging plasma and catalysis synergism, mechanisms involved and highlighted current research development in selective ammonia generation. Finally, we outlined the ways to achieve cleaner and sustainable ammonia production and challenges in future work.

Contents

* Corresponding author.
E-mail address: xuehua.zhang@ualberta.ca (X. Zhang).

https://doi.org/10.1016/j.cej.2024.154920
Received 27 May 2024; Received in revised form 1 August 2024; Accepted 16 August 2024
Available online 19 August 2024

1. Introduction

Hydrogen (H_2) as an energy source has grabbed much attention for achieving net-zero emission [1,2]. However, difficulty for hydrogen liquefaction technology, high diffusive and flammable characteristics, transport and storage challenges remain the critical bottlenecks [3,4]. For instance, liquefaction alone is highly energy intensive as 1 kg production in current electrolyzer requires 50–56 kWh of energy input that leads to 26–30 kg of CO_2 emissions [5]. Alternatively, several chemical energy carriers having high energy densities such as ammonia have been proposed [6]. Ammonia offers several advantages in terms of facile storage, transportation which can also be produced by renewable energy sources like water electrolysis, wind, and solar energy [7].

Ammonia (NH_3) is one of the most important chemical products in human life [8]. It is primarily used for fertilizer production, making its great contribution to sustaining the growing global population [9,10]. In tandem, NH_3 has emerged as an energy carrier due to its remarkable hydrogen content (17.6 wt%) and prominent volumetric hydrogen energy density (3 kWh g^{-1}) [11,12]. Its facile liquefaction either using compression (1 MPa) at room temperature (1 MPa at 298 K) or through chilling to 240 K at ambient pressure (0.1 MPa) allows its easy storage, transportation, and distribution at grid scale energy-effective and cost-affordable [4,13]. Therefore, green synthesis of NH_3 is a global focal point, aiming not only to maximize the agricultural yield but also to serve as an energy carrier in pursuit of carbon neutrality.

Currently, nearly all of the globally manufactured NH_3 (~200 million tons per year) is produced from N_2 and H_2 via the Haber–Bosch (H–B) process which is heavily reliant on fossil fuels [14]. After optimization over a century [15], the H–B process has outperformed and outcompeted other existing processes in terms of energy consumption, such as the Birkeland–Eyde process using electrical arcs, and the Frank–Caro cyanamide process (Fig. 1a) [16]. However, these methods have a massive carbon footprint and therefore, an alternative and sustainable technology is highly desirable.

Cold plasma-assisted technology has been pursued for green NH_3 production which is presumably one of the most environment-benign and cost-effective methods available [17]. Plasma technology has the ability to generate highly energetic electrons, vibrationally-excited species and radicals enabling the break the highly stable triple covalent N_2 bonds (bond energy 946 kJ mol^{-1} due to a large molecular orbital energy gap of 10.82 eV) (Fig. 1b) [18]. Coupling with an appropriate technique (for example, electrochemical nitrogen oxide reduction reaction - NO_xRR), the generated NO_x/NO_x^- species can be converted into targeted NH_3 at a high reaction rate through thermodynamically feasible reactions (Fig. 1c) [19,20]. Cold plasma technology readily interfaces with renewable energy sources, facilitating the synthesis of green NH_3 suitable for both agricultural fertilization and energy applications (Fig. 1c). Moreover, nitrogenous compounds present in agricultural run-off represent viable precursor species for plasma-assisted ammonia production. However, there exist certain limitations in the field of plasma-assisted ammonia synthesis, such as relatively low selectivity, yields and competitive reactions [21]. Nevertheless, this technology still exhibits huge potential for effective nitrogen fixation representing the frontier for sustainable and eco-friendly NH_3 synthesis.

Off late, there has been an upsurge in the review articles discussing ammonia synthesis. The majority of them summarize the state-of-the-art, methods such as chemical and electrochemical, detailing the mechanistic insight and the contribution of catalytic materials design for performance enhancements [4,17,22–24]. A few have archived the plasma related studies for NH_3 synthesis via NO_x reduction [1,25,26]. However, cold plasma-assisted NH_3 synthesis via NO_x has huge potential and deserves intensive exploration. Meanwhile, there are uncertainties in the prospects of uninterrupted NO_x/NO_x^- inflow that can be significant for NH_3 production. In this context, cold plasma-assisted technology is a promising and sustainable approach for producing NO_x at mild conditions forging the clean pathway towards ammonia synthesis. Within this scope, we aim to timely review the current understanding and status of cold plasma-assisted NH_3 production by consolidating research findings in the recent literature.

Herein, we first shed light on whether plasma-activated NO_x synthesis can be a feasible pathway to fix the nitrogen into ammonia. Then we will highlight the synergistic action in the plasma-catalysis method to achieve NH_3 synthesis under mild conditions. Our discussion will also highlight the unique reaction characteristics and mechanisms in the presence of a catalyst leading to enhanced ammonia production with low energy consumption. Then the reader is familiarized with different types of plasma processes for nitrogen fixation. We also identify the underpinning mechanism that leads to improved selective NH_3 production in plasma-assisted technology. Finally, we will try to overview energy consumption and propose renewable energy-based plasma-assisted nitrogen fixation technology at the large-scale level that has a low carbon footprint. We will also discuss the opportunities and challenges.

2. Challenges in ammonia production by conventional and recent processes

2.1. Haber-Bosch process

As discussed, the current global demand for ammonia is met by the conventional H–B route, wherein the ammonia is synthesized through chemical reactions of N_2 with H_2 (Eq. (1)) [4].

$$N_2 + H_2 \rightarrow 2NH_3 \qquad (\Delta H_{298\ K} = -92\ kJ\ mol^{-1}\ N_2) \tag{1}$$

In 1908, the H–B technique was successfully established at large-scale industrial applications as N_2 fixation process [27]. Along with the essential requirement of pure feed gases provided by steam reforming and air separation methods (Eq. (1)), this process also requires high temperature (400–500 °C) and works at high pressure (~30 MPa) in the presence of iron-based mixed oxide catalysts [28] (Fig. 2a). An optimized, commercial H–B plant can produce ~2000 tons NH_3/day, and the efficiency of the process is known to decrease upon downsizing. Conventional H–B process has a theoretical minimum energy input of 22.2 GJ /ton-NH_3 which subsequently produces 1.2 t-CO_2 /ton-NH_3 [29].

Despite optimization efforts, the large-scale swinging temperature and pressure result in high energy consumption (1%–2% of the global energy) and emission of about 1.5–3.1 ton-CO_2 /ton-NH_3 leading to the generation of almost 500 million tons of CO_2 in a year [30]. The 80% of the energy consumption was majorly related to the H_2 formation.

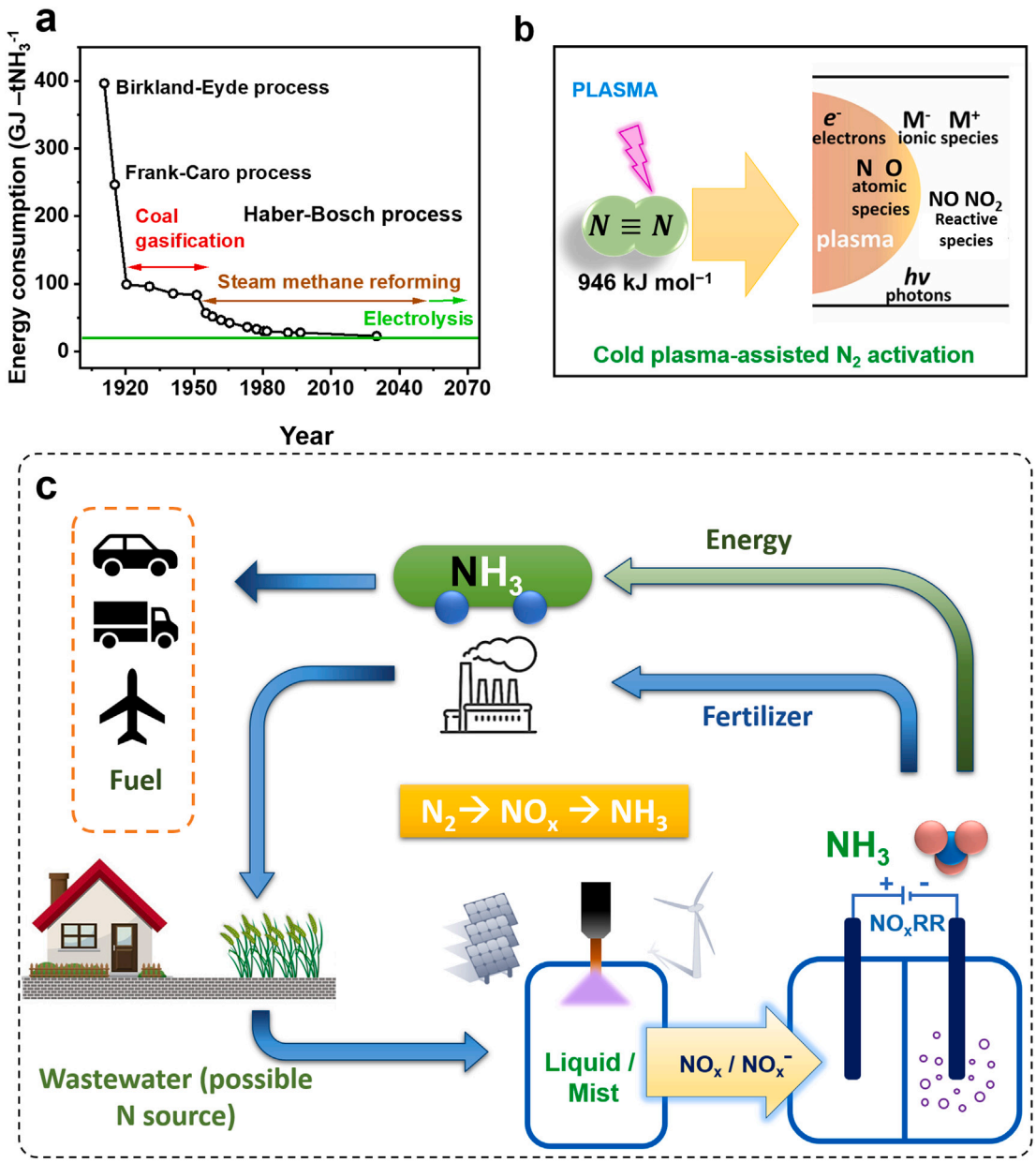

Fig. 1. (a) Progress in nitrogen fixation processes and their energy consumption profile. The green line indicates the theoretical minimum energy consumption (20.1 GJ t-NH_3^{-1}) [16]. (b) Cold plasma-assisted activation of stable N_2 molecule forming reactive nitrogen species in plasma zone [18]. (c) Illustration of emerging cold plasma-assisted catalytic pathway for NO_x/NO_x^- generation and its coupling with electrochemical methods for facile NH_3 production. The synthesized NH_3 can be utilized for agricultural fertilization and energy applications.

Such threats to the environment surged the need for renewable energy-based H_2 production which is also linked with the future hydrogen society [31]. However, if production of NH_3 is carried out by the renewable energy-based H_2 source, such a typical plant's production would be merely <10 tons NH_3/day which is almost 200 times less than the conventional H–B process [1].

An appropriate catalyst during thermal catalytic ammonia synthesis can offset this enormous kinetic barrier and can bring the thermodynamically suitable conditions [32]. Breakthrough in the catalyst development facilitated the dissociation of strong N≡N triple bond by back donation of d-electrons from transition metals into the Π antibonding orbital of N_2. On the other hand, chemical looping synthesis offers opportunities for NH_3 production at low-temperature via hydrogenation or hydrolysis reactions (Eqs. (1) and (2)) [33].

$$N_2 + H_2O \rightarrow 2NH_3 + 3/2O_2 \qquad (\Delta H_{298\ K} = 765.6\ kJ\ mol^{-1}\ N_2) \quad (2)$$

2.2. Electrochemical methods

By far, most research efforts have been devoted to exploring the electrochemical processes for nitrogen fixation and ammonia synthesis. Initially, a direct approach under strict environmental conditions (gas-tight stainless steel autoclave, high N_2 pressure of 50 atm) using Li as a mediator was explored for NH_3 generations [37]. Since then, this method has evolved to a great extent in order to achieve sustainable ammonia production. For example, direct electrochemical nitrogen reduction reaction (eNRR) operated under mild conditions (ambient), eliminating the dependency on pure hydrogen with water electrolysis as an alternative, feasible for delocalized production and distribution has been explored [38–40]. Lately, extensive research has been conducted in this field, due to its compatibility with syndicate renewable energy sources (Fig. 2b) [34]. A continuous-flow reactor is a typical design representing an electrochemical cell that uses an electrolyte

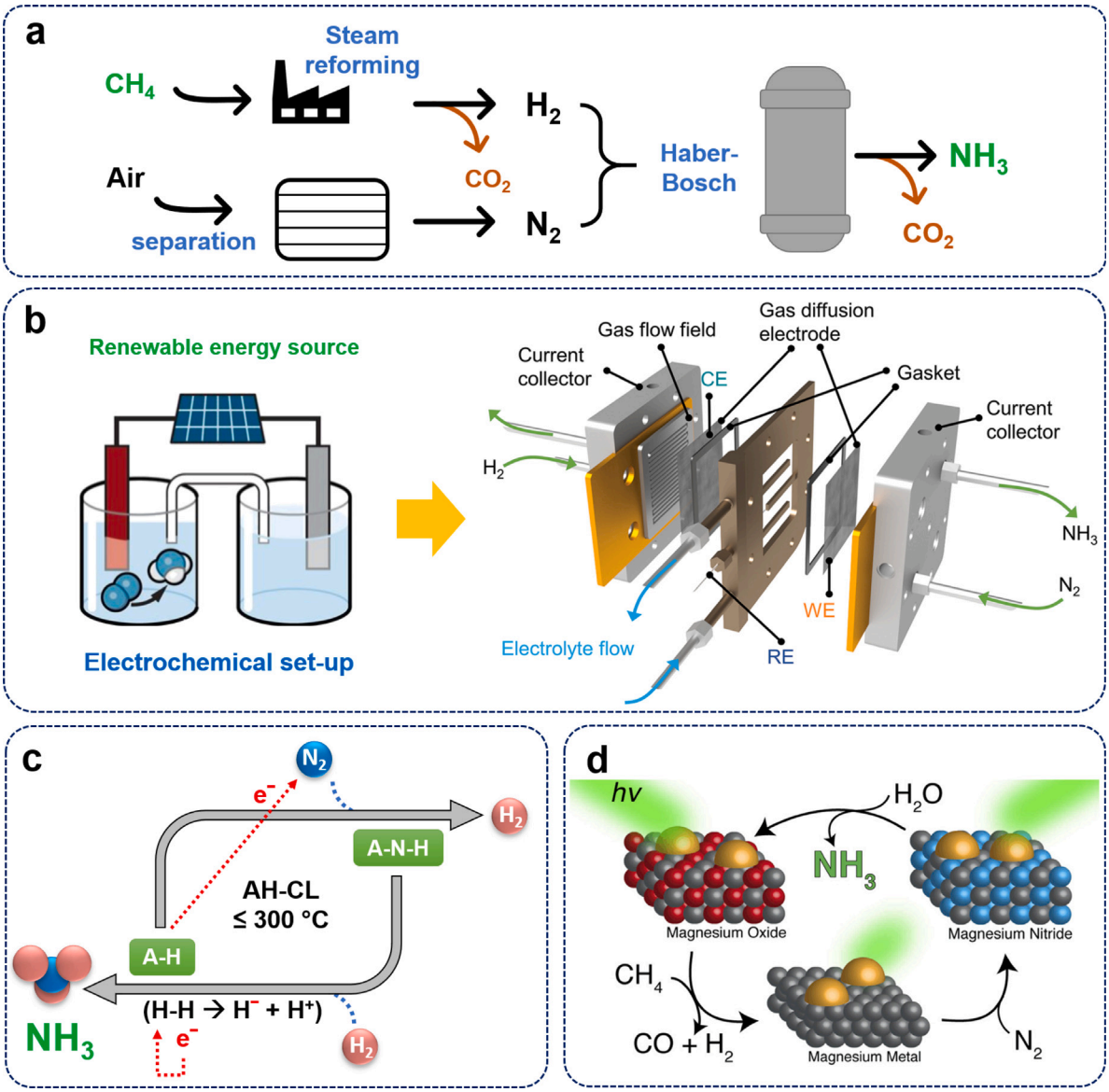

Fig. 2. (a) Schematic illustration of Haber–Bosch process in nitrogen fixation into ammonia [34]. Steam reforming for H_2 production and air separation for purified N_2 are the key steps that eventually produce CO_2 and lead to high energy consumption. (b) Electrochemical set-up run via renewable energy for nitrogen transformation reaction [35]. The figure on the right demonstrates the expanded view of the continuous-flow electrochemical configuration. Nitrogen and hydrogen gases are directly fed into the electrolyte interface to react and NH_3 is collected at outlet. (c) Alkali earth metal hydride (AH) used in chemical loop process (AH-Cl) which reacted with N_2 forming A-N-H [33]. In the next step, A-N-H undergoes the hydrogenation reaction that produces NH_3 and regenerates AH. Electron flow is indicated. (d) Overview of MgO assisted chemical looping which undergoes reduction reaction after reacting with CH_4 and produces Mg metal that combines with N_2 to yield Mg_3N_2. The produced Mg_3N_2 yielded NH_3 after hydrolysis and restored MgO for the looping process to continue [36].

chamber where gaseous reactants could be directly fed to one side of the electrode while electrolyte was fed on the other side and NH_3 is collected after their reaction (Fig. 2b) [35]. Despite these advantages, eNRR is intrinsically limited by its ineffectiveness in breaking the stable N_2 and highly competitive adverse hydrogen evolution reaction (HER) occurring in the same potential window at faster reaction kinetics [41]. While the NH_3 yield rate which typically ranges from $<10^{-4}$ to $<10^{-11}$ mmol s^{-1} cm^{-2}) at variable Faradaic efficiency (50%–100%), a complex set-up and conditions are essentially required to achieve high efficiencies [42]. Additionally, low solubility of N_2 in aqueous solution may lead to low NH_3 selectivity and scalability [34,43]. Therefore, these methods alone has become stagnated and cannot achieve competitive NH_3 synthesis [44].

The electrochemical methods are attractive due to their feasibility for onsite NH_3 production which significantly can eliminate the transportation cost. However, low yield of ammonia and contamination are the major drawbacks. Recently, Li-mediated nitrogen reduction has been reported with 100% of faradic efficiency while it has industrially relevant current densities have also been achieved [42,45]. However, to compete with H–B process, significant work is still needed in this field [46].

2.3. Alkali and alkaline earth metals for NH_3 generation

Application of alkali and alkaline earth metal hydrides (AH) and imides (ANH) has been extensively studied for NH_3 generation which is generally associated with the chemical looping process. In this process, hydridic H from AH reacts with nitrogen and forms ANH [33]. The formed ANH undergoes hydrogeneration via disproportionation of dihydrogen producing NH_3 and regenerating AH (Eqs. (3) and (4)) (Fig. 2c).

$$4/xAH_x + N_2 \rightarrow 2/xA_2NH + H_2 \quad (3)$$

$$2/xA_2NH + 4H_2 \rightarrow 4/xAH_x + 2NH_2 \quad (4)$$

These step-wise reactions can possibly facilitate the NH_3 synthesis that is hard and can only be achieved in thermo-catalytic processes [4]. It should be noted that ANH may convert to nitride, amide, nitride hydride, or nonstoichiometric compounds under certain reaction conditions [47]. Interestingly, the AH mediated chemical loop can be catalyzed by late 3d metals such as Ni, Co, Pd, Ru, etc. In such a combined process of transition metal and alkaline earth metal, the scaling relationship of metal-catalysis can be overcome facilitating ammonia synthesis with high activities at lower temperatures [48]. The AH (Li, Ca, Sr, Ba, Mg) as a strong reducing agent removes the N atom from metal or its nitride and provides an immediate H atom to form ANH_2 (eg, $LiNH_2$) which splits H_2 heterolytically to give off NH_3 [47,49]. It was estimated that, with addition of LiH at 573 K the ammonia synthesis rates are enhanced by up to 3 to 4 orders of magnitude in comparison to bare catalyst [50]. Recently, plasmon-assisted magnesium-based nanomaterial was utilized in a chemical looping. In a cyclic reaction pathway, the MgO was reduced to Mg which upon combining with N_2 yielded Mg_3N_2. Finally, the as formed Mg_3N_2 is hydrolyzed to yield NH_3 and restore MgO for subsequent reaction loop (Fig. 2d) [36].

Increasing efforts have also been observed in Li-mediated electrochemical nitrogen reduction reaction (LiNRR) which aimed to produce NH_3 at renewable energy harvesting sites [51]. Such a method, is usually conducted in ethanol containing nonaqueous electrolyte and catalyst (as working electrode) leading to nitridation, protonation and electro-reduction of Li metal to form NH_3 [52]. Li and co-workers systematically investigated that at 20-bar N_2, a small amounts of O_2 (0.5 to 0.8 mol%) in the feed gas enhanced the FE of up to 78.0 ± 1.3% with 11.7 ± 0.5% of energy efficiency [53]. Recently, it is argued that such lithium-mediated nitrogen reduction reaction methods can effectively produce NH_3 even in ambient conditions (25 °C, 1 bar), while low intrinsic energy-efficiency (up to ~28%) remains a challenge [54]. Overall, the inclusion of alkali metal offers a suitable strategy for ammonia synthesis via electron-rich N_xH_y intermediates.

Furthermore, there are several other scientific and technical challenges making reliable detection troublesome. Since, the amount of NH_3 produced is usually so small, it is challenging to firmly attribute its generation from electrochemical nitrogen fixation process rather than contamination from surroundings. For instance, ambient air contains non-negligible concentration of NH_3 ranging from 0.05 to 250 part per million (ppm), human breath contains 0.3–3.0 ppm which may accumulate in the experimental set-up and interfere with the detection [55]. Even the high-purity N_2 gas may also contain content of NH_3 or NO_x. There can be other sources of contamination such as separating membrane or electrolyte which may release ammonium ions (NH_4^+) or from the catalyst itself [56,57].

While these experimental artifacts are being recognized, concerted attempts are also being made to develop benchmarking protocols for eliminating the sources of contamination. Andersen and co-workers, developed a rigorous procedure using quantitative isotopic measurements that enabled to reliably detect and quantify the electrochemical reduction of nitrogen to ammonia [55]. It is anticipated that such methods can help to prevent false positives from appearing in the literature reporting erroneously high reported faradaic efficiency (FE), and ultimately aid in the development of more efficient processes that yield substantially larger amounts of ammonia. In other cases, passing the feed gas through appropriate adsorbent and control experiments with argon may limit the almost inevitable contamination of the feed gas [58].

3. Cold plasma technology and its assistance in ammonia production

It is evident that there are several challenges that are being observed during the synthesis of NH_3 using existing technologies. The direct N_2 fixation into NH_3 reaction kinetics is sluggish and the energy requirement to activate inert N_2 is relatively high. Assistance of cold plasma technology can overcome such challenges. In general, plasma activation involves the application of electrical discharge that selectively heated the constituting feed gas electrons (e^-) due to their small mass, which upon excitation collides with neighboring gas molecules (O_2, N_2, CO_2, etc.) leading to their ionization and dissociation [59]. The resultant excited species (ions, radicals) participate in subsequent reactions and form new molecules. Therefore, thermal nonequilibrium is developed between the as-formed energetic e^- (approximately of few eV, i.e., several 10 000 K) and the gas molecules (at room temperature). Consequently, localized and highly reactive environment-like conditions were created that led to the proceeding of thermodynamically unfavorable chemical reactions such as splitting of ultra-stable N≡N bonds [60]. Plasma activated N_2 or air and H_2 then form reactive species such as N_2^+, N_2^*, N atoms, H atoms and H_2^+ which subsequently reacts among each other and form NH_3.

Since plasma chemistry can dissociate the highly stable N≡N bonds, attempts have been made for its use as NH_3 synthesis [17,61]. Additionally, there are several positive impacts of plasma-assisted technology as a viable alternative for ammonia synthesis and nitrogen fixation: (i) feasibility to operate under ambient environmental conditions eliminating swinging in temperature and pressure requirements, (ii) it can be easily coupled with any renewable energy, (iii) theoretically, the cost of the energy for plasma-assisted nitrogen fixation is estimated to be the lowest among contemporary technologies, and (iv) it does not release greenhouse gases into the environment.

Ease of operation and coupling with renewable energy sources meets the decarbonized NH_3 synthesis target [62]. It is worth noting, that electricity-powered plasma discharge can be easily turned on/off, and therefore its integration with an intermittent supply of renewable electricity sources is more befitting [63]. The facile operation makes it decentralized in contrast to the centralized H–B process. Furthermore, there are many more advantages which will be discussed in detail in the later sections.

Cold plasma can be mainly classified as low-pressure plasmas and non-equilibrium atmospheric pressure plasmas. Atmospheric plasmas are of interest due to their characteristic discharge playing a major role in surface reactions. Nevertheless, due to the high absolute number density of reactants, higher production rates and number densities of nitrogen fixation can be achieved compared to thermal and low-pressure plasmas [23].

Initial attempts for N_2 fixation into NO_x and NH_3 were related to the use of glow discharge in 1929 [64] after which the subsequent decade witnessed the development and utilization of other types of discharges. Afterward, radio frequency and microwave plasma became the major focus (1989) [65] for NO_x and NH_3 production which were followed by recent dielectric barrier discharge (DBD) systems [26]. Each of these plasma types exhibits a different discharge profile, power consumption and maintains their own distinct discharge zone with different reactor configurations leading to different results in nitrogen fixation. Amongst all, radio frequency (RF) and microwave (MW) typically work at sub-ambient pressures and exhibit elevated gas and electron temperatures, therefore considered as thermal plasma. As a result, a notable concentration of atoms and excited species can be achieved, albeit with a reduced species density [66]. Consequently, these plasmas have a higher capacity to augment the reactant conversions facilitating ammonia synthesis, while bringing low energy efficiency (0.01 to 0.3 g-NH_3/kWh) [67]. Furthermore, operating RF and MW plasmas at higher power densities may entail heightened energy consumption.

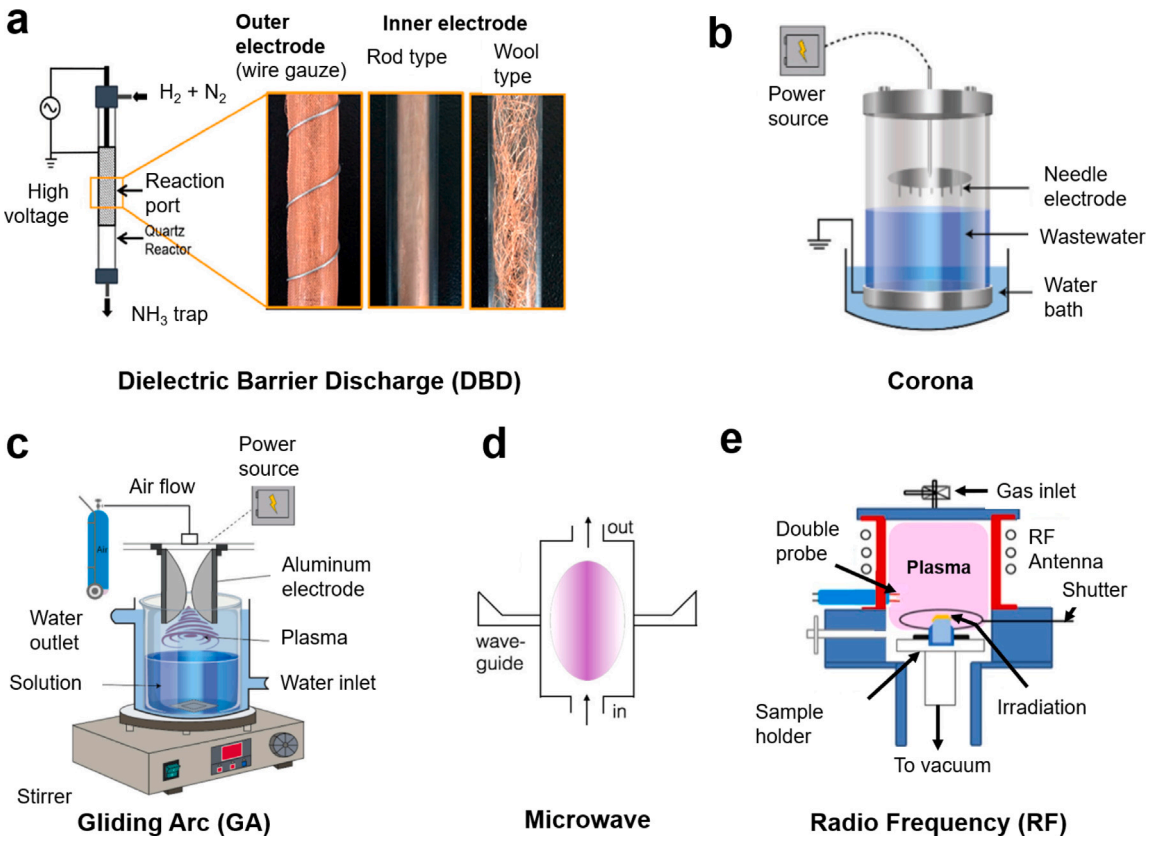

Fig. 3. Schematic diagrams of (a) DBD reactor and image of outer mesh ground electrode and copper wool high-voltage electrode [23]. (b) Corona discharge set-up with circular metallic plate as the ground electrode and tungsten needles as high-voltage electrode [70]. (c) GAD reactor containing two symmetric aluminum electrodes placed on a magnetic stirrer and retrofitted with water circulation for temperature control [70]. (d) MW plasma set-up [1]. (e) Radio-frequency plasma reactor [71].

Recent investigations showed that pulsed discharge systems can foster the non-equilibrium plasma state which in turn can facilitate the yielding of comparatively lower gas temperatures exhibiting higher reactivity at minimal energy input. For instance, the adoption of pulsed discharge over continuous modes amplified the ammonia energy efficiency within an RF reactor up to 7.7 g-NH_3/kWh [68]. However, in the continuous mode reactor, the produced ammonia has enough time to diffuse back into the plasma discharge zone and undergo dissociation via electron impact. Therefore, the pulsed mode is considered to be a better option as it extinguishes the plasma before ammonia diffusion and enhances ammonia synthesis concurrently consumes less energy [67].

Apparently, a reverse correlation between N_2 fixation and energy consumption is seen in the literature. Minimizing the energy input is often accompanied by a low N_2 fixation. As of now, DBD plasma system stands out for its operation at atmospheric pressure, which lends it a high degree of production. The versatility of modulating the voltage magnitude, and discharge current has been found crucial for high energy conversion rate. However, the formation of microdischarges and their uneven distribution may affect the consistency of the reaction [69]. Besides DBD reactors, plasma generated under low-pressure conditions using microwaves has also been proven to accelerate ammonia synthesis. Unlike the DBD reactor, microwave plasma can also generate spatially and temporally uniform plasma. Yet again, microwave plasma systems suffer from high energy input power. Various studies for this purpose with the reported efficiency and energy consumption are summarized in Table 1 (NO_x) and Table 2 (NH_3). An overview is presented in the following section discussing the types of plasma reactors for enhanced NO_x production.

(a) *Dielectric barrier discharge (DBD)*: The DBD plasma approach is one of the most commonly used technologies presumably due to its simplified reactor design (a continuous reactor) (Fig. 3a) [95]. It is operated at atmospheric pressure by applying an AC potential difference between two electrodes wherein one of electrode is covered by a dielectric barrier. The high breakdown voltage at atmospheric pressure provides the narrower discharge gaps and volumes compared to low-pressure plasmas. Despite exhibiting lower ionization rate in DBD reactor, the cumulative population of ionized and excited species at atmospheric pressure exceeds that at low pressure [67]. The simple design of DBD reactors makes them suitable for large-scale applications and therefore has been implemented in industries such as ozone synthesis [96]. Contrarily, the energy efficiency for nitrogen fixation at large-scale is still low.

Furthermore, DBD plasma systems are feasible to couple with catalytic a catalyst preventing the arc discharges from damaging the catalyst surface [26]. More electrons are generated through this process, causing electron avalanches to form discharge channels. For such reasons, energy efficiency in DBD plasma can sometimes be enhanced. Consequently, the system is extensively explored for ammonia synthesis and nitrogen fixation. For example, a DBD reactor packed with different catalyst support materials (α-Al_2O_3, γ-Al_2O_3, TiO_2, MgO, $TaTiO_3$, and quartz and Cu wool) was tested for NO_x production wherein the best results were obtained with a γ-Al_2O_3 catalyst [73]. Adaptations like metal-based wool or rod catalysts as inner electrode and wire gauze as outer, have also been introduced while the basic configurations remain the same as shown in Fig. 3b [23]. However, the obtained energy cost was high (18 MJ/mol N) and the product yield was low (0.5 mol%) due to presence of excessive energetic electrons which in led to dissociation instead of vibrational excitation [1].

Roy and co-workers found that the modification of DBD reactor (electrode gap over water surface) improved the distribution of microdischarge that not only resulted in the selectivity (98% for NO_3^-) but

Table 1
Overview of nitrogen fixation and energy consumption for various plasma configurations.

Plasma configuration	Yield	Energy consumption
Nitrogen oxide (NO_x) species		
Spark discharge [72]	1% NO_x	2.41 MJ/mol
Packed DBD γ-Al_2O_3 [73]	0.5% NO_x	18 MJ/mol NO_x
Pulsed milliscale GA [74]	1% NO_x	10 kWh/kg NO_x
Transient spark discharge [75]	NO, NO_2	8.6 MJ/mol N
Sliding plasma discharge [76]	NO (160–1040 mg/L)	24–67 MJ/mol NO
ns-pulsed spark discharge [77]	NO, NO_2	5–7.7 MJ/mol NO
RGA plasma reactor [78]	5.5% NO_2	2.5 MJ/mol
GA plasma [79]	1.5% NO_2	3.6 MJ/mol NO_x
ns-pulsed spark discharge [80]	NO_x yield at ca. 1.35 mmol/h	–
GA + MW plasma [81]	8670.2 μg/mL NO_2^-	–
DBD/Spark discharge [82]	1.62% NO_x	6 MJ/mol
DBD TiO_2 [83]	24.5 mg/L NO	266.1 GJ/t-N
Spark discharge [84]	1.8%–3% NO_x	1.9–4.4 MJ/mol
DBD + 3-stage spark discharge [85]	4500 μmol/min NO_x^-	25.66 MJ/mol
High frequency spark discharge [86]	1.25% 1.65% NO_2	6.1 MJ/mol
DBD [86]	0.25% NO_x	38 MJ/mol
Pulsed plasma jet [87]	0.02% NO_x	0.42 MJ/mol N
Pulsed milli-scale GA [88]	1%–2% (NO and NO_2)	2.8–4.8 MJ/mol
Rotating arc plasma [89]	5.8% NO_x	2.38 MJ/mol
Liquid-phase bubble pin-plate spark discharge [90]	11.17 μmol/min	39.22 MJ/mol
Reverse vortex flow GA [91]	2.4%	2.21 MJ/mol
Plasma jet [92]	0.52% (NO_2^-) and 1.2% (NO_3^-)	–
DBD MnO_x/Al_2O_3 Packed-Bed [93]	0.42 standard cm^3/min	0.016 MJ/mol
MW [94]	3.8% NO_x	2 MJ/mol

also reduced the energy cost to 20.7 MJ/mol NO_x [97]. Further, to cut down the energy requirements, a solar-driven DBD with a 3-stage spark discharge (a form of thermal plasma) design was employed in series to achieve high yield and low energy consumption of plasma-water-based nitrogen fixation [85]. Therefore, changing the reactor configurations can modulate the performance of DBD system for enhanced nitrogen fixation with simultaneously low energy consumption. Choosing the right catalyst, and packing material to prevent the NH_3 decomposition and to reduce the discharge power required to ignite the plasma are a few modifications that may be the future research avenues.

(b) *Corona discharge*: In this discharge system, a high-voltage electrode ionizes the surrounding air and/or liquid which leads to the generation of localized charged free electrons, ions and radicals are generated. The configuration usually have ground (metallic plate) and high voltage electrode (needles) (Fig. 3b) [70]. Jose et al. (2019) also designed a pulsed CD reactor using a circular metallic plate as the ground electrode and 7 tungsten needles connected to a high-voltage power supply [98].

(c) *Gliding Arc (GA) discharge*: Among the initial technologies, the GA plasma are characterized by reduced electric fields below 100 Townsend (Td), providing electron energies ~1 eV. The presence of such electrons is of great use for vibrational excitation of the secondary gas molecules. These excited electrons were generated in a pulsed-power milliscale GA reactor and used for NO_x formation [88]. The discharge produced is considered to be in a transition regime, which crosses the boundary between non-thermal and thermal plasma. The discharge is usually formed as thermal but transforms into a non-thermal one via space and time evolution [99]. In terms of reactor configuration, it has not changed much yet. It usually contains two symmetrical electrodes connected to high voltage forming an electric arc in cycles which in turn generates the reactive species (Fig. 3c) [70]. The N_2 fixation through these processes was estimated to be most promising as up to 2% NO_x concentration was achieved with 2.8 MJ/mol of energy cost [79]. Recently, new approaches resulted in NO_x concentrations up to 5.9% bringing down the energy cost up to 2.1 MJ/mol [100].

(d) *Microwave (MW) discharge*: In terms of yield and energy consumption, microwave (MW) -based plasma may be promising but is categorized as thermal plasma type. The MW-based plasma is created by applying MWs, i.e., electromagnetic radiation with a frequency between 300 MHz and 10 GHz to a gas, without using electrodes (Fig. 3d) [1]. The gas flows through MW in a quartz tube intersecting with a rectangular waveguide, absorbs the energy, and forms the discharge. A pulsed MW plasma at reduced pressure produced ~6% of NO without catalyst at an energy cost of only 0.60–0.84 MJ/mol NO. Such astonishing results are due to the dominance of energetically favorable vibrational-induced dissociation of N_2 [1]. The yield was further improved (14% NO) energy cost was reduced (0.30 MJ/mol NO) which is so far the best performance for MW plasma achieved at low pressure under the magnetic field. However, these results have not yet been reproduced since they were reported back in 1980 [79]. Recently, Bai et al. produced the NH_3 from methane and nitrogen using the cobalt and cobalt–iron supported on gamma alumina ($\gamma - Al_2O_3$) catalysts [101].

(e) *Radiofrequency (RF) discharge*: The RF-based plasma excitation has been used decades ago, and has recently gained substantial attention. The RF reactor configuration typically exhibits radio frequency as a source of energy which is applied to a gas, often at low pressure, that leads to the generation of a warm plasma state (Fig. 3e) [71]. Various metals such as Fe, Cu, Pd, Ag, and Au were used to form meshes along with gallium in RF plasma which resulted in the energy yield of 0.22 g-NH_3/kWh and with a maximum yield of ~10% at 150 W [102]. The dominance of NH_2 formation on the catalyst surface was found to be the major reason for higher NH_3 production. One of the recent reports also showed comparable nitrogen fixation efficiency (>8%) while maintaining a hydrogen-rich surface configuration [68]. The mechanistic insight revealed that in the absence of H, nitrogen atoms quickly recombine, and nitrogen molecules desorb from the surface which in turn limit the N_2 fixation into ammonia. Briefly, a variety of plasma reactors (and discharge types) can be applied for the NO_x and NH_3 generation from N_2 [18] (see Table 2).

4. Plasma-assisted single-stage pathway for ammonia synthesis ($N_2 + H_2 \rightarrow NH_3$)

4.1. Non-catalyzed NH_3 synthesis

Some of the early work showed that the variation in nitrogen–hydrogen ratios led to the formation of NH radicals, hydrogen atoms, and hydrogen molecules which supposedly are indispensable for NH_3 synthesis [65]. One-step synthesis of ammonia was achieved at the water surface by creating the reaction locus between a plasma phase

Table 2
Overview of NH_3 formation and energy consumption for various plasma configurations.

Ammonia (NH_3) synthesis		
Modern H–B [103]	10%–15% NO_x	0.49 MJ/mol
DBD MgO+glass pellets [104]	0.57%	576 MJ/mol
DBD carbon coatings on α-Al_2O_3 [105]	1.2%	576 MJ/mol
DBD MCM-41 as catalyst [106] α-Al_2O_3	3.75%	27 MJ/mol
DBD with wool-like metal electrodes [107]	3.5%	93 MJ/mol
Catalytic DBD Ni/Al_2O_3 [108]	0.77%	115.4 MJ/mol
DBD Ni/Al_2O_3 [109]	1.4%	103.7 MJ/mol
Membrane DBD Ru/Al_2O_3 [110]	4.62%	154.7 MJ/mol
DBD PZT [111]	2.7%	68 MJ/mol
DBD PZT [112]	7%	–
Ni/Silica - $BaTiO_3$ in DBD [113]	12%	81 MJ/mol
DBD Rh/Al_2O_3 [114]	1.43%	65.11 MJ/mol
DBD [115]	0.3%	58.85 MJ/mol
DBD with MOF (ZIF-8/67) [116]	–	12 kJ/L
Plasma jet - Co_3O_4 [117]	39.6 mg/cm^2/h	–
DBD MgO-mesoporous silica/Ni [118]	4.4 mmol/h/g_{cat}	–
10Ni/zeolite 13X in DBD reactor [119]	1.25%	44 kJ/L
Pt/BaO/Al_2O_3 Plasma reactor [120]	>1%	4.61 MJ/mol
CoNi-MgO DBD [121]	12.07 μmol/g/h	2.15 kJ/L
Ni-Co-MOF DBD [122]	88.21 μmol/g/min	–
boron-doped g-C_3N_4 DBD [123]	2.48 mmol/g/h	20.16 kJ/L
Rotational GA [124]	0.4 mmol/min	19 MJ/mol
Ru/MgO DBD [60]	2.67 mmol/h/g_{cat}	4.2 kJ/L
Needle plate plasma [125]	7.67 mg/h	0.68 g/kWh
DBD [126]	3.7 mmol/h/g_{cat}	2 W
Ni/LaOF DBD [127]	34.94 μmol/min/g_{cat}	31.2 kJ/L
Fe-laser induced plasma [127]	70.8 μmol/g/min	–
Ru/CeO_2 DBD [127]	6.8 mmol/g/h	–

(gas phase) and a water phase (liquid phase) in the presence of UV light [128,129]. It was proposed that the plasma phase abstracts hydrogen from water that transiently formed NH, which is then reduced to NH_3 and UV energy promotes the dissociation of atoms in plasma gas. Catalyst free electrolytic approach led to key hydrogen radical formation at plasma-water interface by action of solvated electrons which in turn produced direct NH_3 [130].

The addition of ethanol (20%) in aqueous media and its subsequent exposure to air as a source of N_2 plasma jet enhanced ammonia production from 0.2 to 3.2 mmol/L [131]. It was justified that, increasing the ethanol content in the aqueous matrix delivers more hydrogen which makes the nitrogen reduction more facile rather than its oxidation which in turn improved the NH_4^+ production.

Similarly, an in-situ synthesis method was developed using an advanced spray-type jet plasma under UV exposure, which significantly fixed the nitrogen in the form of several NO_x species (nitrate, nitrite) and co-synthesized ammonium at the liquid interface at a high rate (2.5 μmol min^{-1}) [132]. It is important to note that, the reaction mechanism differs in the presence and absence of UV exposure. During the plasma phase, N atom, N_2^* and nitrogen ions (N_2^+) can be produced while N_2^* and N_2^+ are much active than N atom [133]. The active N_2^* and N_2^+ species then react with UV-mediated dissociated •H and •OH species producing N-containing products different from ammonia. On the other hand, UV exposure did not promote the reactions associated with the N atom and therefore, an enhanced NH_3 production was achieved with higher selectivity. Such results showed that the presence of UV irradiation provides additional hydrogen donors which subsequently improves NH_3 production. Also, the reaction at liquid interface starting from N atom and those starting from N_2^* and N_2^+ follow different mechanisms.

While the single phase or direct plasma-assisted NH_3 synthesis is possible, the undifferentiated oxidative attack by plasma can result in the formation of undesired products and dissociation for formed NH_3 molecules [24]. Aqueous phase reactions that are usually performed in the presence of H_2O, such as plasma-assisted N_2–H_2O for NH_3 formation suffers several challenges, including low yield and selectivity. In such a case, the direct formation of targeted product NH_3 may lead to formation of other oxidized species. For instance, plasma fixation in aqueous phase produced nitrogen oxidized species at higher concentration while NH_3 remained as low (0.2 μmol/mL) in comparison to NO_x (3.5 μmol/mL) (Fig. 4a) [134]. This occurred due to the oxidative attack of the OH or H_2O_2 species present in water solution or mist which play an important role in the nitrogen fixation end product. Despite this, the approach holds great potential as an alternative to traditional methods of ammonia production [135].

4.2. Plasma-catalysis for enhanced NH_3 synthesis

Combining plasma with catalyst (plasma-catalysis) has demonstrated a significant improvement in the performance of many gas conversions, including ammonia synthesis due to the synergy between the plasma and the catalyst [23,108,140].

4.3. Selection and design of catalysts

An appropriate catalyst in the plasma-catalyst system is vital for nitrogen fixation as NH_3 however, its selection requires a fundamental understanding of plasma-catalyst interactions. Various catalysts such as Ru, Mg, Cu, Co, Fe, Ni and their derivatives (oxides) in the form of pellets or powder have been extensively explored for ammonia synthesis [17]. The challenge is to identify catalytic descriptors determining the activity and selectivity of catalytic materials in plasma-based reactors. The Sabatier principle has provided a conceptual justification for deciding the optimum catalyst that explains: the catalyst with intermediate strength towards reactant is the ideal [137]. Metals binding too weakly (for example, ruthenium, copper, nickel, etc.) restrict the N_2 dissociation while that bind too strongly (for example, Fe, Mo., etc.) show limited desorption of atomic N and other N-containing intermediates exhausting the availability of binding sites and hindering the reaction rate.

The introduction of tungsten (W) catalyst increased NH_3 production up to 24% while the absence seems relatively lower [141]. It was demonstrated that the presence and absence of the catalyst can substantially modulate the production rate. The catalyst not only improved the production rate but also shifted the maximum of production to 50% of initial N_2 fraction. It is proposed that this difference could be attributed

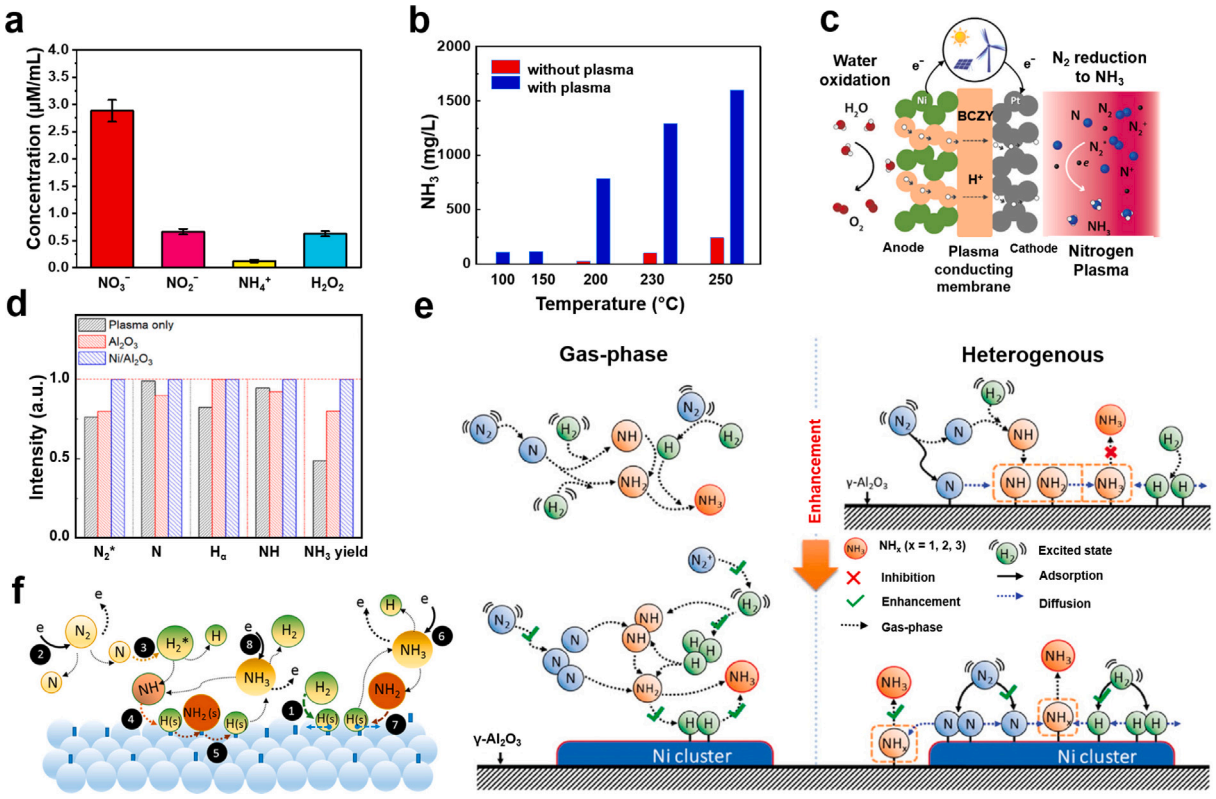

Fig. 4. (a) Concentration of aqueous RONS in water aerosols after passing through the plasma array [134]. (b) Effects of exposure of plasma on ammonia production in a packed-bed DBD plasma reactor with Ru-Mg/γ-Al_2O_3 [31]. (c) Plasma-solid oxide combination for enhanced transportation of proton for ammonia synthesis at cathode [21]. (d) Comparison of plasma alone and in combination with Al_2O_3 and Ni/Al_2O_3 packing for NH_3 production [108]. (e) Possible reaction mechanism of plasma ammonia synthesis over a solid catalyst [4]. (f) Predominant chemical pathway for (step 1–8) NH_3 synthesis based the kinetic modeling of atmospheric-pressure plasma system [136].

to the possible adsorption of plasma-activated N and H atoms on W surface in the gas phase forming NH_3 via intermediate NH radical.

Similar combinatorial effects of plasma and catalyst, Ru–Mg/ γ - Al_2O_3 pellets were shown wherein the ammonia production increased from 10 mg/L to 810 mg/L when plasma was switched on with energy yield of 25–30 g of NH_3/kWh (Fig. 4b) [31]. The catalyst Ru-Al_2O_3 was used in the fluidized bed plasma reactor which showed the higher energy yields (5.9 NH_3/kWh) than the conventional packed-bed DBD reactor [142]. The accelerated effect was due to the increased contact area between the plasma and scattered catalyst particles in the fluidized bed plasma reactor. Realizing the potential of synergistic action of plasma and catalyst, a proton concentrating methodology was adopted where reactive H could easily react with the plasma-activated nitrogen for ammonia synthesis. To achieve this, an in-house built proton conducting membrane composed of commercial half-anode supported cell Ni-BCZY/BCZY (where BCZY is catalyst derived different elements such as Ba, Ce, Zr, Y and O) with a Pt cathode is introduced for accelerated reaction of reactive species for higher NH_3 production (Fig. 4c) [21].

An affordable and efficient Al_2O_3 supported Ni catalysts - Ni/Al_2O_3 was tested in plasma catalysis wherein the normalized relative intensities of N_2^+, N, Hα, and NH was higher than that of only plasma, and Al_2O_3 (Fig. 4d) [108]. The obvious generation of NH radicals in the plasma led to the initiation and acceleration of ammonia synthesis. Generation of gas-phase NH radicals fostered the selective production of NH_3. Based on such results, a plausible reaction mechanism revealed the formation of NH_3 can follow various pathways (Fig. 4e).

In general, exposure to plasma can generate several reactive species including dissociated atoms such as N and H, ions like N_2^+, H_2^+, vibrationally and electronically excited molecules (N_2^* and H_2^*) that can participate in either gas-phase or on the surface of the catalyst [4]. The presence of catalyst like Ni/Al_2O_3 can improve both kind of reactions. To further understand these pathways, a schematic given in Fig. 4f can be taken into consideration [136]. It is given that plasma and catalysis combination led to the (1) formation of hydrogen H(s) and (2) atomic nitrogen through the dissociative excitation adsorbed on the surface of the catalyst, which further reacts with H_2^* (3) and form NH radical. Consequently, (4) a reaction between H(s) and NH leads to the generation of surface-adsorbed NH_2(s) which results in the formation of (5) NH_3 by Langmuir–Hinshelwood (L–H) reactions mechanism (explained later). However, there may be (6) NH_3 dissociative reactions occurring which forms NH_2 radical. The dissociated NH_3 further interacts with atomic H(s) again (7) and recycled NH_3 through the surface interaction. An (8) alternative pathway of the dissociation of NH_3 may also occur. Detailed plasma reactors, reaction mechanisms for catalysts, and effects from feeding sources can studied in the review published by Gharahshiran & Zheng, 2024 [67].

Density functional theory (DFT) calculation indicates the NH_3 synthesis is highly dependent on the adsorption energies of N atom on the metal surface [143]. Assuming the first key step for N_2 fixation starts with rate limiting dissociation of N_2 (Eqs. (5) and (6)) [4,137]. Both, theoretical as well as experimental study explains that the rate is determined by the energy barriers: the transition-state energy (activation barrier) for N_2 dissociation (E_{N-N}) (determining the rate of dissociation) and the adsorption energy of nitrogen (E_N) (determining the coverage on the surface) [144]. It has been demonstrated that active metal catalysts facilitate this reaction. Consequently, a scaling relationship can be formed determining the catalyst selections with lower N binding energy and with a lower N_2 dissociation barrier as overlaid on the plot given in Fig. 5a [137]. Based on such observation, a "volcano" type curve was developed for different metals indicating their binding strength for ammonia synthesis (Fig. 5b) [145]. The catalyst on the left side of the curve indicates their strong N binding efficacy facilitating easy dissociation of N_2 while the catalyst on the right side of the curve has weak binding affinity indicating limitations

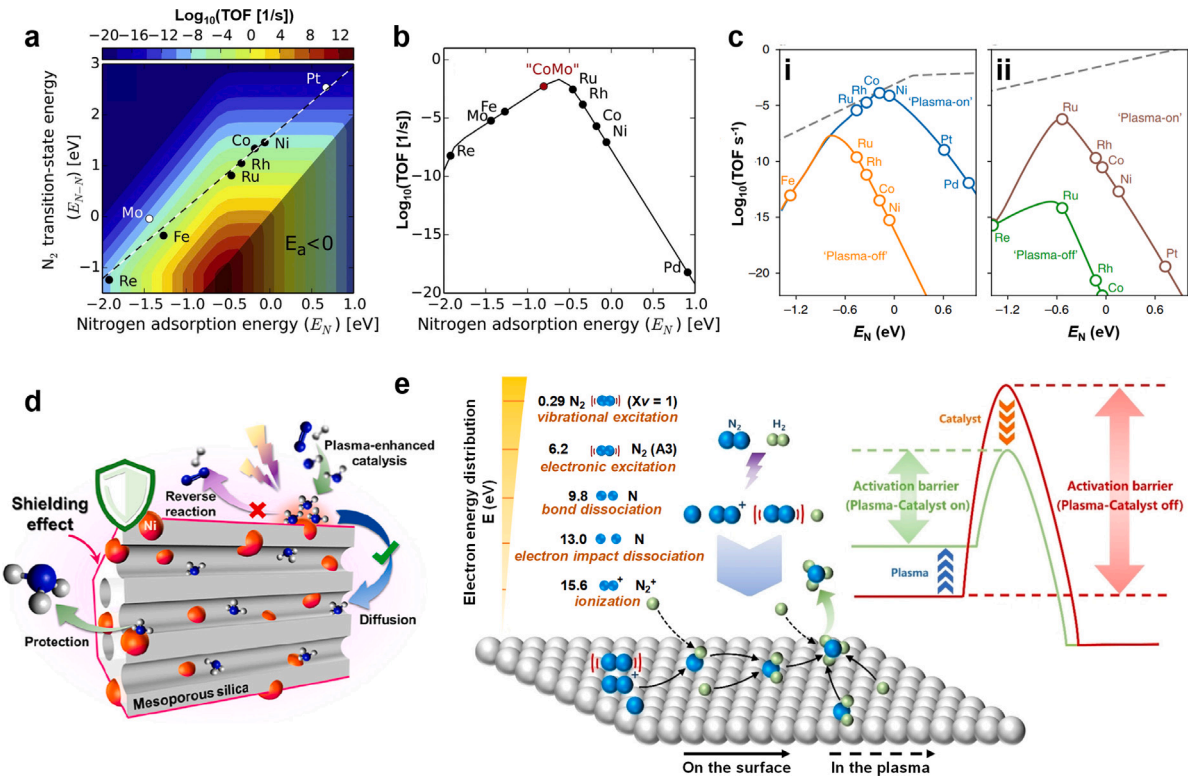

Fig. 5. (a) The plot showed the NH_3 synthesis rate as a function of N_2 adsorption energy and N_2 dissociation barrier with energetics for FCC/HCP metal step sites and scaling line. Shaded area shows the theoretical limit since the activation barrier (E_a) must always be positive. (b) Turnover frequencies (TOF) for ammonia synthesis as a function of the adsorption energy, utilizing that E_{N-N} is a linear function of E_N. Based on the interpolation between the two N adsorption energies, "CoMo" marked as a red dot appeared at top for NH_3 synthesis activity [137]. (c) Rate enhancements with plasma-induced N_2 vibrational excitation and comparison with the thermal catalytic i.e., plasma-off (i) terrace an (ii) sites [138]. (d) Schematic of simultaneous formation of NH_3 in a plasma-assisted surface reaction and the "shielding protection" effect on mesoporous MCM-41 catalyst [139]. (e) Synergistic effects of plasma and catalysts in plasma-catalyzed synthesis of ammonia synthesis [26].

for nitrogen dissociation due to a high nitrogen dissociation barrier. As already explained, catalysts with intermediate binding strength for N are optimum for carrying the NH_3 production, osmium and ruthenium were found to be the most active metal catalysts while a bimetallic CoMo has been kept at the top [145].

While a catalyst provides surfaces influencing the recombination reactions, as well as consecutive reactions, it is not limited to just surface reactions. The complexity of the interaction between plasma and catalyst is severe, as any change in the catalyst will induce changes in the plasma, which again can influence the catalyst. It is also crucial to restrict the counterproductive as there are high chance of reverse reaction that can lead back to reactants. At the same time, several materials can enhance the reaction pathways for ammonia production preventing reverse reactions. By selecting suitable catalysts that interact with various species at specific sites, plasma catalysis can enhance the yield and selectivity of ammonia synthesis.

$$N_{2(g)} + 2^* \rightarrow N - N^* + ^* \rightarrow 2N^* \quad (5)$$

$$N^* + 3/2H_{2(g)} \rightarrow NH_{3(g)} + ^* \quad (6)$$

4.4. Synergy of plasma with catalysts

Coupling with cold plasma action can initiate N_2 activation in the gas phase even before adsorption onto a catalyst surface. Based on the theoretical calculations, plasma-on and plasma-off (indicating thermal catalytic process) conditions on catalyst step (Fig. 5c i) and terrace site (Fig. 5c ii) were compared [138,146]. The presence of plasma can initiate the vibrational excitation of N_2 molecules which decreases N_2 dissociation energy barrier on catalyst different sites indicating that ammonia synthesis scaling relations can be overcome. Therefore, it can be predicted that the ammonia synthesis can be enhanced for metals that bind atomic nitrogen weakly on the catalyst surface (high E_N), given that N_2 activation is usually the rate-limiting step for ammonia synthesis. New findings can open more room for improvements in the process via careful control of plasma-catalysis properties [147].

Yet again, the hybrid plasma-catalytic process still suffers from plasma-induced reverse reaction of NH_3 decomposition via electron impact dissociation [8]. To solve this issue, Wang and coworkers proposed a "shielding protection" generating from carefully designed Ni/MCM-41 bespoke mesoporous catalyst in DBD reactor which significantly limits the plasma-induced NH_3 decomposition (Fig. 5d) [139]. Uniquely, the absence of plasma discharge in the internal mesoporous feature of the catalyst not only protected the evolved NH_3 with "shielding protection" but also enabled high NH_3 yields of >5%. These advancements were indeed effective and may be used in future for overcoming many challenges associated with N_2 fixation using plasma-catalysis process.

4.5. Plasma-catalytic reaction mechanisms: Eley–Rideal (E–R) and Langmuir–Hinshelwood (L–H) reactions

To further predict the reaction to a certain extent, it is important to underpin the mechanism of plasma–catalyst interactions [148]. This interaction of plasma and the catalyst is not straightforward, however occurs typically through the Eley–Rideal (E–R) and Langmuir–Hinshelwood (L–H) reactions [26]. The E–R reaction involves the individual reaction of active particles with the catalyst surface, resulting in the products continuing to be adsorbed on the catalyst. In this case, one reactant is activated by the catalyst. In contrast, the L–H reaction occurs when both active particles involved in the reaction are adsorbed on the catalyst, and both reactants are activated in the presence of the catalyst. The NH is one of the most vital intermediate species during the

activation which regulates the NH_3 yield, is predominantly formed via the E–R reaction that adsorbed onto the catalyst surface (Eq. (7)) [149].

$$N_{(s)} + H \rightarrow NH_{(s)} \quad (7)$$

$$NH_{(s)} + H_{(s)} \rightarrow NH_{2(s)} \quad (8)$$

$$NH_{2(s)} + H_{(s)} \rightarrow NH_{3(s)} \quad (9)$$

$$NH_{2(s)} + H \rightarrow NH_{3(s)} \quad (10)$$

The as-formed NH species may further react to H species and form NH_2 and NH_3. Conversely, NH_2 radicals are predominantly formed via hydrogenation of NH free radicals, and their generation is governed by the L–H reaction, as shown in the reaction (Eq. (8)). Hydrogenation of NH or NH_2 to NH_3 is less likely to occur, while its formation may take either of the pathways [L–H (Eq. (9)) or E–R (Eq. (10))]. However, at a higher pressure, E–R reactions are predominant [102]. Dissociative reactions may also occur that may reverse the reaction and form NH_x and H (or H_2 and NH_3) reducing overall yield (Eqs. (11) and (12)). Therefore, it is crucial to achieve a balance between formation and decomposition for an effective ammonia synthesis process.

$$NH_3 + e^- \rightarrow NH_2 + H + e^- \quad (11)$$

$$NH_3 + e^- \rightarrow NH + H_2 + e^- \quad (12)$$

Furthermore, plasma-catalyzed NH_3 synthesis is also affected by factors like reaction conditions, catalyst characteristics and plasma environment. Co-existence of plasma and catalyst influences their mutual interactions and may affect the conversion of N_2 and/or H_2. Nevertheless, the synergy of plasma with different catalysts is capable of dissociation of N_2 at lower energy input and can supplement the NH_3 production as shown in Fig. 5(e) [26]. Briefly, plasma interaction forms the active excited species that are subsequently adsorbed on the catalyst surface where they may further excite the secondary molecules. Availability of active sites on catalyst surface provides favorable reaction conditions for these reactions, lowering the dissociation energy barrier and promoting interactions between reactant molecules for enhanced NH_3 production. However, the formation of microdischarges on the catalyst surface can shift the reaction pathways from gas phase to the catalyst surface. Concerns have also been raised for the lifetime of plasma-activated species and their sufficient transportation to the catalyst surface to prevent species recombination. Therefore, the synergism between plasma and catalysts remains elusive, and a multidisciplinary approach is needed.

5. Two-stage pathway of ammonia production via $N_2 \rightarrow NO_x \rightarrow NH_3$

Researchers have turned to an alternative two-stage pathway beginning with the oxidation of N_2, followed by catalytic reduction of the resultant NO_x species to NH_3 [150]. Shifting to such a pathway is due to the facile formation of plasma-assisted NO_x/NO_x^- species. Reduction of these plasma-assisted NO_x/NO_x^- is thermodynamically more favorable and thus can proceed in a wide potential window without HER interference. Notably, low dissociation energy would be required if NO_x/NO_x^- are used as precursor due to their N=O bond containing low bond energy (204 kJ mol^{-1}) in comparison to break the N≡N triple bond that leading to better NH_3 production kinetics.

Coupling with electrochemical and electrocatalytic processes represents the current research frontier to achieve superior ammonia synthesis performances [23,151]. Plasma-assisted formation of more reactive NO_x^- followed by electrochemical reduction is recognized as much easier if compared to direct NRR in terms of selectivity and rate kinetics [34,152]. It can be attributed to the more positive standard reduction potential (E°) of NO_3^- reduction (0.69 V versus reversible hydrogen electrode, vs. RHE) than that of N_2 reduction (0.093 V vs. RHE) which again confirms that NO_x conversion is thermodynamically easier than N_2 [153]. Therefore, two-stage catalytic approaches reducing NO_x/NO_x^- in to NH_3 are considered to be promising than other catalytic approaches [154]. Plasma-assisted NO_x production such as NO, NO_2, NO_3 and so forth have been extensively explored which strongly suggests its feasible integration in NH_3 synthesis process.

5.1. First stage: Plasma-assisted production of NO_x from N_2

5.1.1. Discharge condition for NO_x production

A low-frequency window in spark discharge exposure provided a continuous increase in the NO_x production while the energy requirement remained constant (Fig. 6a). A further increase in the discharge frequency (kHz) at a large scale led to a drastic improvement in NO_x production while the cost of energy was reduced by almost 2.6 times (Fig. 6b). Such higher production was attributed to the significant contribution of vibrational excitation and the use of the residual species at higher frequencies [84]. Exposure to plasma does not only produce NO_x species but a bunch of several other reactive species. While the generation of other species may represent the non-selective nature of plasma, co-production of H_2O_2 can improve the plasma-induced NO_x concentration. This happens due to the higher solubility of NO_x species in an acidic solution. Therefore, the production of H_2O_2 can elevate the solubility of nitrogen species in aqueous media increasing its overall concentrations. Similar observations were obtained where the concentration of selective NO_3^- increased continuously in spark discharge mode (warm plasma), while NO_2^- and H_2O_2 concentrations reached a plateau after 5 min. Such a pattern indicates a balance between H_2O_2 production and its subsequent consumption in the production of NO_3^- (Fig. 6c) [155].

Several other approaches have been explored to improve the concentration of NO_x via plasma assistance. For example, longer plasma exposure linearly increased the NO_x (NO_3^- and NO_2^-) concentration reaching ca. 1.35 mmol h^{-1} dictating the improving effects of extended discharge (Fig. 6d) [80]. The role of specific energy input was also highlighted where an increase in energy at optimized operation conditions led to enhanced generation of NO_x species [156] (Fig. 6e). In fact, the innovation behind the input of higher energy is the transfer of large energy to energetic electrons. These energetic electrons transfer the energy and excite other molecules that further lead to cascading discharge effects and improve the faster chemical reaction for NO_x production. Exposure of plasma at elevated pressure also led to improvement in the NO_x production rate. This was observed in a rotating gliding arc system operated at elevated pressure (3 bar; gauge pressure) that resulted in a dramatic improvement in NO_x yield (69 g/h) with high selectivity (94%) for NO_2 at lower energy consumption (Fig. 6f) [18]. The higher production of NO_2 in comparison to others was attributed to the (i) elevated gas temperature (ii) reduced back reactions when higher pressure was applied. Despite these concentrated efforts, high NO_x yield at low energy consumption remains debatable because existing methods either require active cooling (consuming more energy), strict operation conditions, or an additional set-up (effusion nozzles) which eventually adds up cost to the system.

5.1.2. Reactant composition

Feeding the pure H_2 directly or indirectly contributes to CO_2 generation because it is usually extracted via methane combustion. Alternatively, water oxidation reactions are an alternative method for H_2 production [157]. Inspired by this, direct use of N_2–H_2O in plasma-assisted ammonia synthesis is being employed. Furthermore, considering the safety challenges associated with explosive hydrogen gas, using H_2O is a safer and more environmentally friendly option [26]. However, it generally suffers from a low yield and selectivity due to the formation

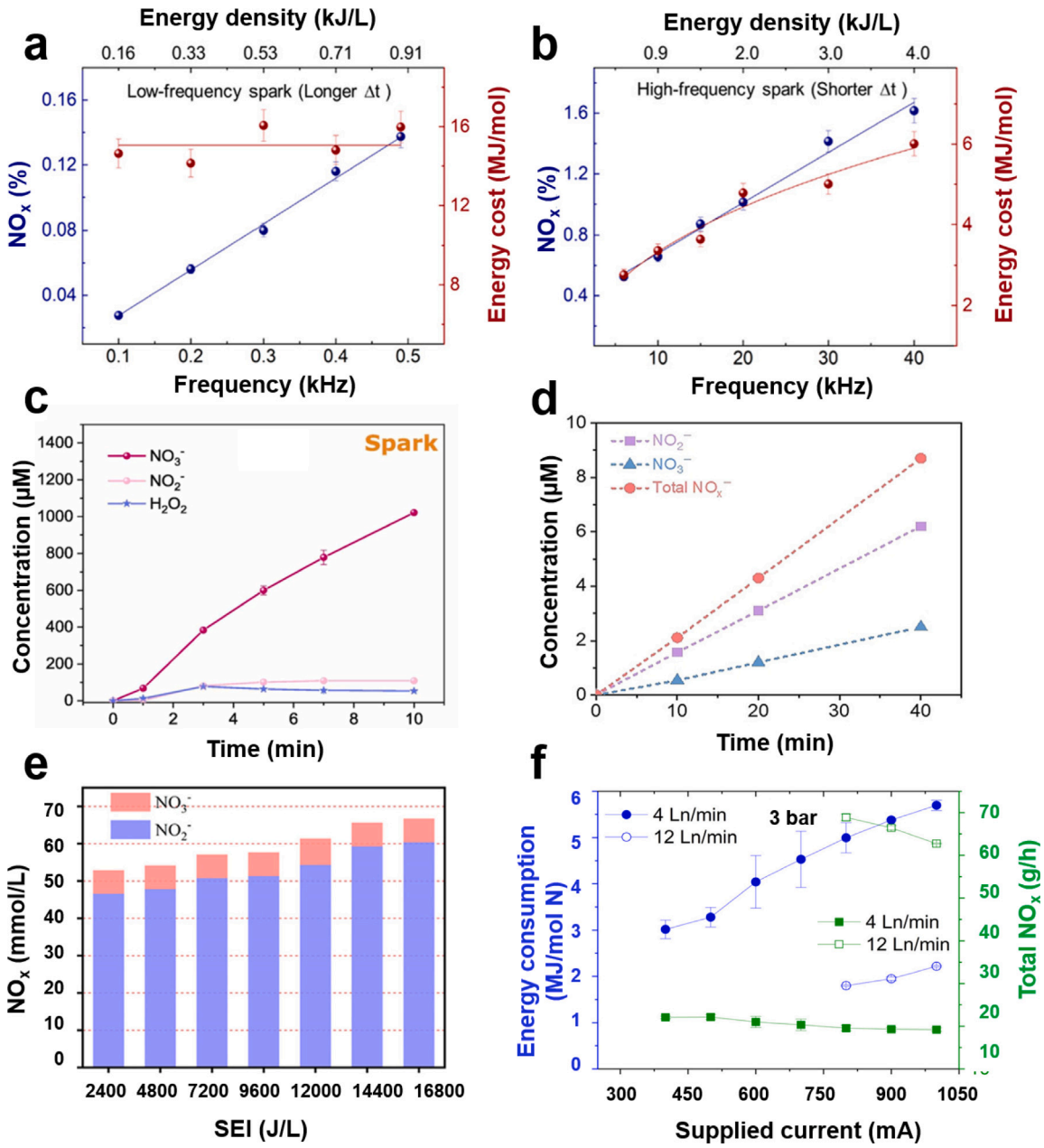

Fig. 6. NO_x concentrations and corresponding energy cost in spark discharge reactor at g = 5 mm: (a) 0.1–0.5 kHz and (b) 5.0–40.0 kHz [84]. (c) Yield of NO_x^- as a function of plasma treatment time [155]. (d) Generation of higher NO_3^- concentration along with co-production and consumption of H_2O_2 and NO_2^- indicating a balance between species in the liquid phase during a spark discharge modes [80]. (e) Concentration of NO_x species increases with the increase in specific energy input (SEI) [156]. (f) Energy consumption for total NO_x production rate at contant gas ratio of N2/O2 1:1, 3 bar (gauge pressure) and flow rate of 4 and 12 Ln/min [18].

of oxidative species, NO_x/NO_x^-. Despite such challenges, this approach holds great potential for concentrating NO_x species.

In general, under the plasma exposure, H_2O and N_2 experiences concurrent oxidation and reduction processes, precipitating the decomposition of H_2O into H atoms and OH radicals. The generated H species derive the reduction reactions for ammonia synthesis, whereas OH participates in the nitrogen oxidation and results in the formation of NO_x/NO_x^- as secondary products [26]. Therefore, the mechanism of N_2–H_2O shares similarities with N_2/H_2 except the additional reactions that led to formation of reactive oxygen-nitrogen species (RONS) [60].

Similarly, using the ambient air as a source of N_2, can leads to the formation of NO_x species as a product [152]. While feeding air instead of N_2 may reduce the dependency on pure N_2 gas, its presence can significantly lower the selectivity towards the overall goal to NH_3. For example, O_2 co-exits with N_2 in air (21%), which leads to the formation of oxygenated long-lived NO_x (nitrate/nitrite) that dominates during the activation process of cold plasma. In particular, oxygen scavenges a large number of plasma-assisted free electrons to transform into excited species which in turn react with N atom and form active NO_x species. Plasma-assisted approaches usually contain N_2^*, H_2^+ wherein reactive oxygenated species promote the NO_x synthesis that is usually difficult to achieve in thermal equilibrium conditions [23,146].

However, controlling the gas flow rate containing H_2O as humidity may shift the process from NO_x for ammonia production in a gas–liquid mixed-phase. For instance, Wang et al. showed that keeping an intermediate N_2 flow rate (30 mL/min) can improve NH_4^+ ion concentration (16.9 mg/L) while the selectivity still remained as low as 25% [125]. Zhang and co-workers showed in a DBD reactor that an increase in the water vapor input flow rate led to an increase in the NH_3 generation rate [60]. Lower flow rate (0.2 to 1.0 L/min) resulted in an increment

of NH_3 production from 1.53 μmol/h to 65.4 μmol/h. Formation of high density vibrationally excited $H_2O(\upsilon)$ led to high reaction rate of dissociative adsorption for H and N for higher production of NH_3. During a plasma jet reactor, an introduction of small amount of H_2O (from 2%–10% saturation) vapor led to higher yield of NH_3 with higher selectivity ca. 96%. Increasing the vapor saturation resulted in a higher production but the selectively suffered largely. Therefore, speculation can be made that a certain concentration of water, specifically in gas form can enhance the overall ammonia synthesis while a higher content, either gas-phase or liquid system leads to NO_x generation and reduced NH_3 selectivity.

5.1.3. Microbubbles for enhanced NO_x production

Dissociation of N_2/air forms reactive oxygen and nitrogen species (RONS) in the plasma zone which can be concentrated in an aqueous medium. Formation of plasma-carrying bubbles, 'plasma-bubbles' and their subsequent diffusion into the liquid phase is one the innovative methods to intensify the gas-to-liquid mass transfer of these reactive species [158,159]. The collapse of the bubble facilitates the on-site release of the plasma-excited gas into the liquid phase, leading to a higher reaction rate in the aqueous phase [160]. With the higher surface area-to-volume ratio, microscopic bubbles speed up the gas transfer at the interface [161–163], and in the presence of solid particles, they exhibit distinct stability compared to their macroscopic counterpart [164,165].

Several configurations to couple the bubbles with the production of a plasma discharge system have been reported [159,166,167]. In one of the configurations, the plasma discharge and bubble formation happen almost simultaneously, reducing the loss of short-lived active species thus enhancing the concentrations of NO_x in the aqueous phase and producing plasma-activated water (PAW) (Fig. 7a) [168]. An alternative underwater bubble-enhanced cold plasma treatment of water is to set up an air-plasma jet at the bottom of a static reactor, where bubbles form through mesh as the jet is generated (Fig. 7b) [169–171]. Except for underwater configuration, a feasible configuration with the plasma needle array closely set above the air–water interface is designed while microbubbles are infused from the external bubble generator (Fig. 7c) [172,173].

To further improve the mass transfer of reactive species within the aqueous system, the plasma discharge system was coupled with a supercavitation device which eliminated the requirement of an external gas cylinder [176]. Another feasible design was to couple the venturi tube to the water loop, and bubbles loaded with plasma formed due to the self-suction of the feeding gas at the neck of the venturi were directly introduced increasing NO_x concentration in the aqueous phase [177]. Recently, plasma discharge coupled with a venturi tube led to the formation of microbubbles for enhanced cold plasma activation (MB-CPA) [174,178]. The configuration was developed by tailoring the 3D-printed venturi tube that controlled the size distribution of microbubbles and enhanced the generation of NO_x species (Fig. 7d). The working distance of plasma-activated bubbles is shortened compared with other reported configurations based on hydrodynamic cavitation, maximizing the concentration of NO_x in the aqueous phase. The improvement in the degradation efficiency of model compounds by several times compared with the same flow without microbubble is the evidence for higher diffusion of reactive species (Fig. 7e) [174,175]. Therefore, MB-CPA in a flow system seems to be promising in the production of NO_x^- at a large scale while its coupling with an appropriate reduction system can also lead to nitrogen reduction reactions.

For ammonia generation, Peng et al. introduce the N_2 bubbles in the aqueous phase under a high-voltage electrode to generate plasma through underwater discharge. A significant ammonia production rate of 11.2 μmol min^{-1} was achieved, however, the selectivity was poor due to obvious co-production of NO_x species [179]. Sun et al. used a hybrid multi-bubble underwater spark discharge reactor that initially transformed the atmospheric air and water into NO_x species under mild conditions [34]. The produced NO_x species were subjected to an electrochemical set-up which successfully reduced the NO_x species to NH_3 . Reviewing the literature, it becomes evident that microbubble discharges intensify the NO_x species in the aqueous phase making them more suitable for the former stage ($N_2 \rightarrow NO_x$) of the two-stage pathway for ammonia synthesis.

While these strategies are effective for NO_x generation, the selective photoreduction of NO_x to N_2 in the presence of catalysts may also occur. The oxygen-rich photocatalyst can capture the O atom in NO to form N_2 at low conversion rates [180]. Recently, DBD plasma reactor was used with a catalyst having oxygen vacancies (OV) which facilitated the adsorption and activation of NO_2, leading to its disproportionation reaction and the generation of N_2O, NO, NO_2 and NO_3^- [181]. The coexistence of OVs and NH_x groups provides a new pathway for converting NO to N_2 by reducing the adsorbed NO_2 and NO_3^-. Similarly, co-existence of NH_3 was found to be favorable for the reduction of NO_x to N_2 at lower plasma discharge power [182]. Continuous removal of NO_x from the reaction mixture could be one of the solutions, but this might not be straightforward in practice [79].

5.2. Second stage: Reduction of NO_x to NH_3

The transformation of NO_x to NH_3 is the next step which is challenging due to the huge number of electron transfers. For instance, conversion of NO_3^- needs an eight-electron transfer reaction and requires lower electrode potential (0.69 V versus the reversible hydrogen electrode (RHE)) [183]. It is also worth mentioning that the potential from going NO_3^- to NH_3 typically requires lower than HER potential (0 V versus RHE) which otherwise results in the undesired consumption of electron donors to produce H_2 leading to low faradic efficiency [184]. Given the large number of proton transfers, 9 and 7 for NO_3^- and NO_2^- reduction, respectively, a large over-potential is needed to achieve the equilibrium between the generation of H (proton) and its timely consumption. Under such conditions, more energy is required and selectivity for NH_3 production also deteriorates [185].

5.2.1. Pathway from NO_x to NH_3

Specific NO_x species such as nitrite (NO_2^-) and/ or nitrate (NO_3^-) are the major product of plasma assisted N_2 activation, reduction to NH_3 follow different routes for production [154]. Nitrate has been extensively explored as a source of nitrogen for the ammonia synthesis process due to its widespread distribution in the environmental matrices as a contaminant [186]. Moreover, high solubility and reduced bond energy of N=O (204 kJ mol^{-1}) and prospects of synchronous environmental remediation (NO_3^- pollutant removal) makes is suitable candidate for a promising and alternative to direct N_2 reduction reaction for NH_3 production [187,188].

Owing to the excellent solubility of NO_x species in an aqueous medium, gliding arc-microwave plasma (warm plasma) was used to produce NO_x first, followed by electrolysis over Cu_2Pd/CBC (carbonized bacterial cellulose). The NO_x species were treated with an alkaline (KOH) solution for generation of NO_x^- species which in turn was subjected to an electrochemical system for ammonia synthesis (Fig. 8a) [189]. Performance evaluation in KOH with and without plasma treatment revealed that the current density is increased from negative onset potential to more positive in plasma-treated 0.5 M KOH, implying more favorable kinetics for reduction reactions (Fig. 8b). Notably, alkaline mediums are characterized by high pH value that renders a positive impact on the selectivity of NH_3 production [190]. Similarly, electrolyte characteristics were regulated to alkaline during a plasma oxidation process that selectively formed NO_2^- species (92.38 ± 1.17%) as major component [44]. The as formed NO_2^- species was then easily transformed into NH_3 using electro-reduction method as six-electron-transfer require less energy compared to the eight in NO_3^- reduction. Such improvements in selective NO_x/NH_3 formation can be attributed to the suppression of HER activity in an alkaline medium. The well-known Volmer step of the HER process in neutral

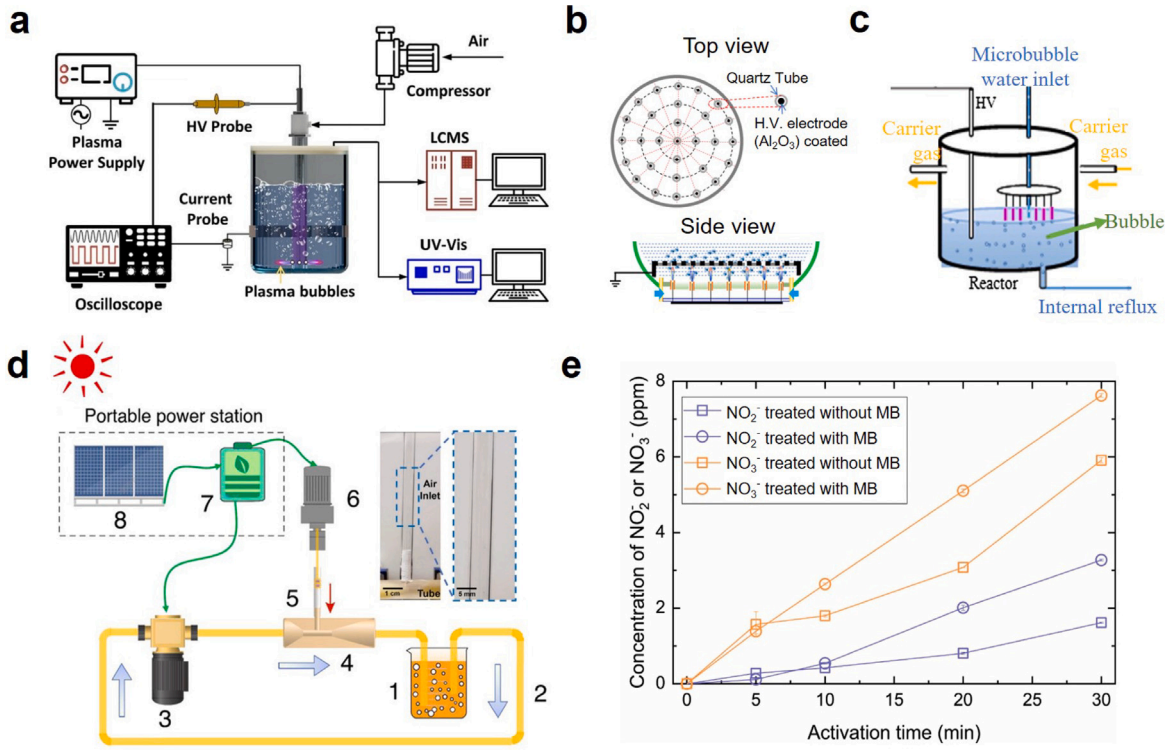

Fig. 7. (a) A schematic experimental setup of the underwater diffuser coupled with DBD plasma reactor [159]. (b) Schematics of setups for underwater bubble generation combined with the microplasma jet array [169]. (c) A microbubble-enhanced multi-needle corona plasma discharge reactor for the degradation of dichloroacetic acid [173]. (d) A schematic of experimental setup for microbubble-enhanced cold plasma activation (MB-CPA) technology, which can be driven by solar energy. An atmospheric corona discharge cold plasma is applied in the set-up [174]. (e) Concentration of nitrite and nitrate ions after the plasma treatment with and without microbubbles (MB) [175].

or alkaline electrolytes ($H_2O + e^- + * \rightarrow {}^*H + OH^-$) involves a prior water dissociation process that features a high energy barrier; this is not the case for that in acidic medium ($H_3O + e^- + * \rightarrow {}^*H + H_2O$) [191]. Therefore, the HER processes in neutral and alkaline electrolytes are more sluggish in contrast to those in acidic electrolytes due to the restricted Volmer step (Fig. 8c).

5.2.2. *Catalysts for NO_x reduction*

In an electrocatalytic study, CuO nanowire arrays showed outstanding ammonia production selectivity (81.2%) and high faradic efficiency (95.8%) [192]. However, conventional Cu-based nanoparticles require high overpotentials (ca. 1.2 V) to obtain practically acceptable yields and faradic efficiency. In fact, bare Cu nanoparticles exhibit low binding affinity and nucleophilicity of NO_x^-, and sluggish water dissociation fails to provide sufficient protons. However, the modified Cu-based material are frequently used in plasma-assisted NO_x reduction investigations [34,151]. For example, Cu/Cu_2O nanoparticles were used in plasma-catalysis approach in an inflow system, NO_3 concentration was selectively increased in a former step, which then subsequently transformed into NH_4^+ in a latter at rate of approximately 30 nmol/s at −0.5 V vs. RHE (Fig. 8d) [155]. In contrast, such a two-stepped transformation to NH_3 was combined together in a single plasma-activated electrochemical set-up and NH_3 was produced at a rate of 26.8 nmol s^{-1} cm^{-2} [21].

Since Ni exhibited strong adsorption for intermediates such as ${}^*NO_3^-$, ${}^*NO_2^-$ and ${}^*NH_2$, it has been carefully coupled with Cu for electrocatalytic nitrate reduction reactions [153]. The HER activity on bare Ni or Cu is strong which can lead to low selectivity and efficiency for ammonia production. Therefore, a modulated catalyst design forming $Cu_{50}Ni_{50}$ was investigated which led to effective reduction reactions and concomitant HER suppression for selective NH_3 production. The catalyst enhanced the NH_3 faradic efficiency by over 20% at compared to pure Cu at different NO_3^- concentrations (Fig. 8e). A high selectivity for NH_3 at a production rate of 198.3 μmol/cm^2/h was achieved with 100% faradic efficiency using a boron-rich core–shell nickel boride nanoparticle [80]. The nitrogen fixation was achieved in two steps, N_2 to NO_x^- through plasma-activation reactor (Fig. 8f) and coupling of electrocatalytic reduction led to high selective conversion of NO_x^- to NH_3 (Fig. 8g). Bimetallic catalyst, $Co–Ni/Al_2O_3$ reduced the total number and intensity of acidic sites on the catalyst surface which facilitates the desorption of synthetic NH improving the yield (1500 μmol/g/h) and selectivity [193]. This combination of two distinct metal-forming Co-Ni bimetal enhances the plasma discharge.

5.2.3. *Optimal selection of NO_x species*

Based on this discussion, the pathways starting from NO_x seem to be effective for NH_3 production, while there exist several challenges. For instance, the process starting from nitrate renders low selectivity as it may also accumulate NO_2^- as a long-term operation [194]. N_2 fixation via a nitrate intermediate requiring huge energy due to its involvement in a change in the nitrogen oxidation state from 0 to +5 and then down to −3 which indirectly interfered with selective NH_3 formation [195]. Keeping this in view, different N-containing species that are easy to undergo reduction reactions may be considered as a solution for enhanced selective NH_3 production. For example, NO_2^- mediated reaction may undergo effective reduction reaction to achieve more practical results for industrial perspectives [196]. Meng and co-workers designed cobaloximes integrating with multi-walled carbon nanotubes (MWCNTs) catalysts with a CoN_4 skeleton [197]. The catalyst was successfully combined spark discharge which showed selective NO_2^- to NH_4^+ transformation at yield of 0.438 mmol. Here, NO_2^- was targeted in order to reduce the huge electron change

Alternatively, changing the precursor from NO_2^- to NO eventually leads to a smaller number of electron transfers for selective NH_3 generation. For example, H_2O splitting through GA plasma led to the co-generation varying H_2/NO which was coupled with catalytic

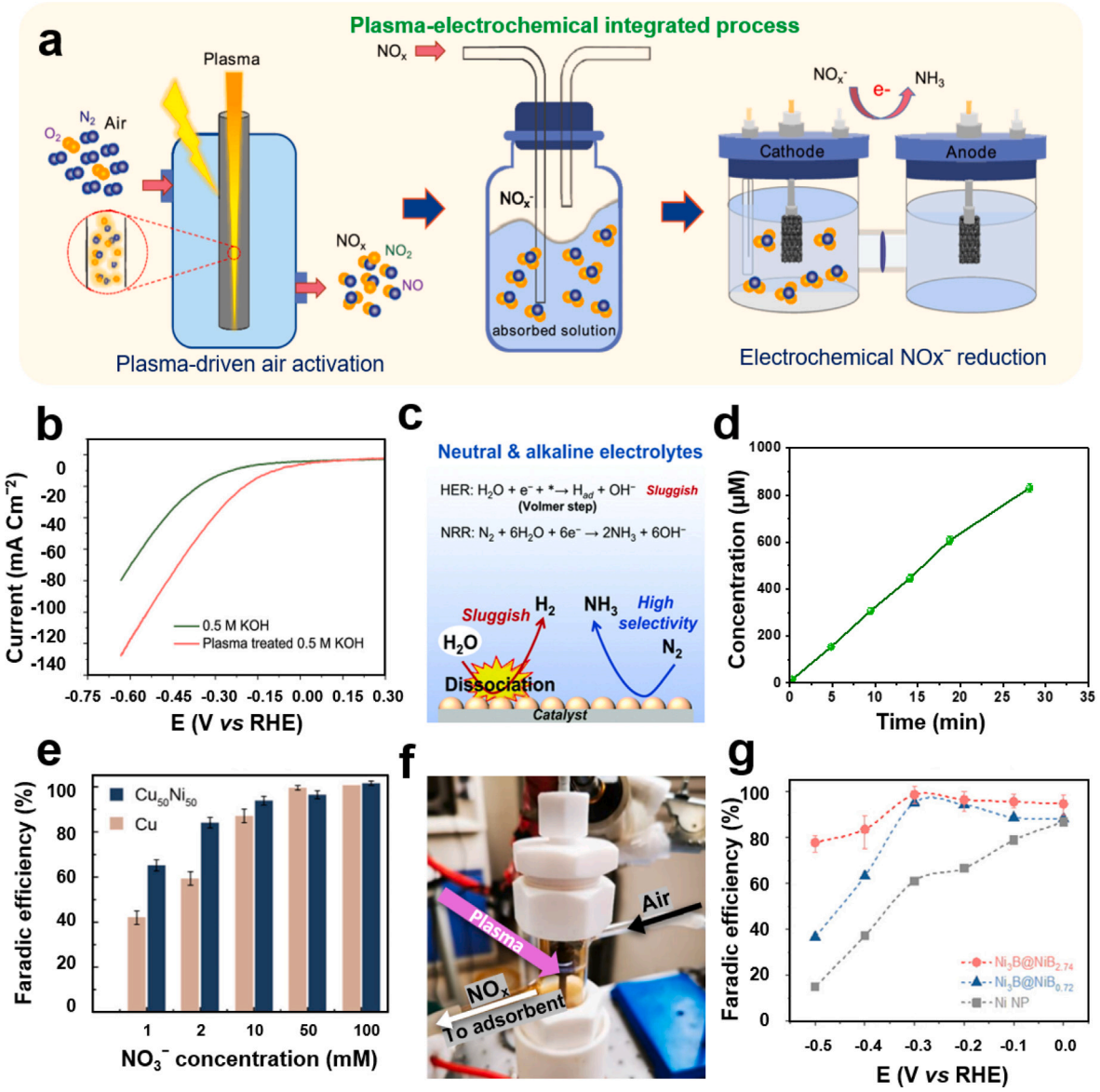

Fig. 8. (a) Schematic indicating two-step strategy with integrated cold plasma assisted electrochemical reduction technique for high-efficiency nitrogen fixation for ammonia production [189]. (b) Linear sweep voltammetry (LSV) of Cu_2Pd/CB pure KOH (0.5 M) and plasma-treated KOH (0.5 M) showing a positive shift in the current density that implies favorable reduction reactions [189]. (c) Sluggish effects in HER processes in neutral and/or alkaline systems that eventually improve NH_3 selection [191]. (d) Ammonia production as a function of time using plasma-activated electrolyte at −0.5 V vs. RHE [155]. (e) Comparison of the highest NH_3 faradic efficiency (FE) on the $Cu_{50}Ni_{50}$ and pure Cu catalysts at different NO_3^- concentrations [153]. (f) Photograph of the plasma reaction chamber. (g) High faradic efficiency NH_3 yield showing a positive relationship with different surface B-rich core–shell nickel borides [80].

reduction that was found to be critical for selective NH_3 production. Increasing the specific energy input (≤7.5 kJ/L), the oxidation of generated NO sharply reduced to 0 which completely transformed to NH_3 with ~95% selectivity [198]. Wang and co-worker also argued that NO may be the major species for selective NH_3 production [150]. During their investigation, NO was selectively introduced to Cu_6Sn_5 based plasma-catalytic process that showed higher selectivity for NH_3 production with 96.9% of faradic efficiency at low overpotentials compared with the Cu and Sn catalysts. The study showed NH_3 production at rate of 10 mmol cm^{-2} h^{-1} which is highest reported value. This study of NH_3 synthesis require two-stage pathway, $N_2 \rightarrow NO \rightarrow NH_3$. Although the major focus has been given to the latter, the former is far less known in terms of its viability. Nevertheless, such plasma-catalyzed processes are still under development and are not yet economically competitive. Currently, our understanding of the reaction mechanism still seems incomplete, and based on experimental findings different explanations for enhancing the selective transformation of $NO_3 \rightarrow NH_3$ have been proposed.

6. Energy consumption

Among the cold plasma-assisted technology, the microwave and DBD reactors have been reported to exhibit higher NH_3 synthesis rate which is usually achieved through combination with heterogeneous catalysis [16]. Fig. 9(a, b) shows a comparison of the energy budget of several plasma processes for nitrogen fixation in terms of NO_x and NH_3 production. The highest energy efficiency that has been achieved so far is, 36 g-NH3/kWh which corresponds to 1.7 MJ/mol of NH_3, in need of promoted ruthenium catalyst [31,201]. If plasma catalysis is to be compared with the benchmark H–B process, considering its low adaptability to downsizing, this yield is still lower by 10-fold. By the direct plasma-catalysis for ammonia production, high NH_3 yield typically consumes high energy while the energy-efficient processes

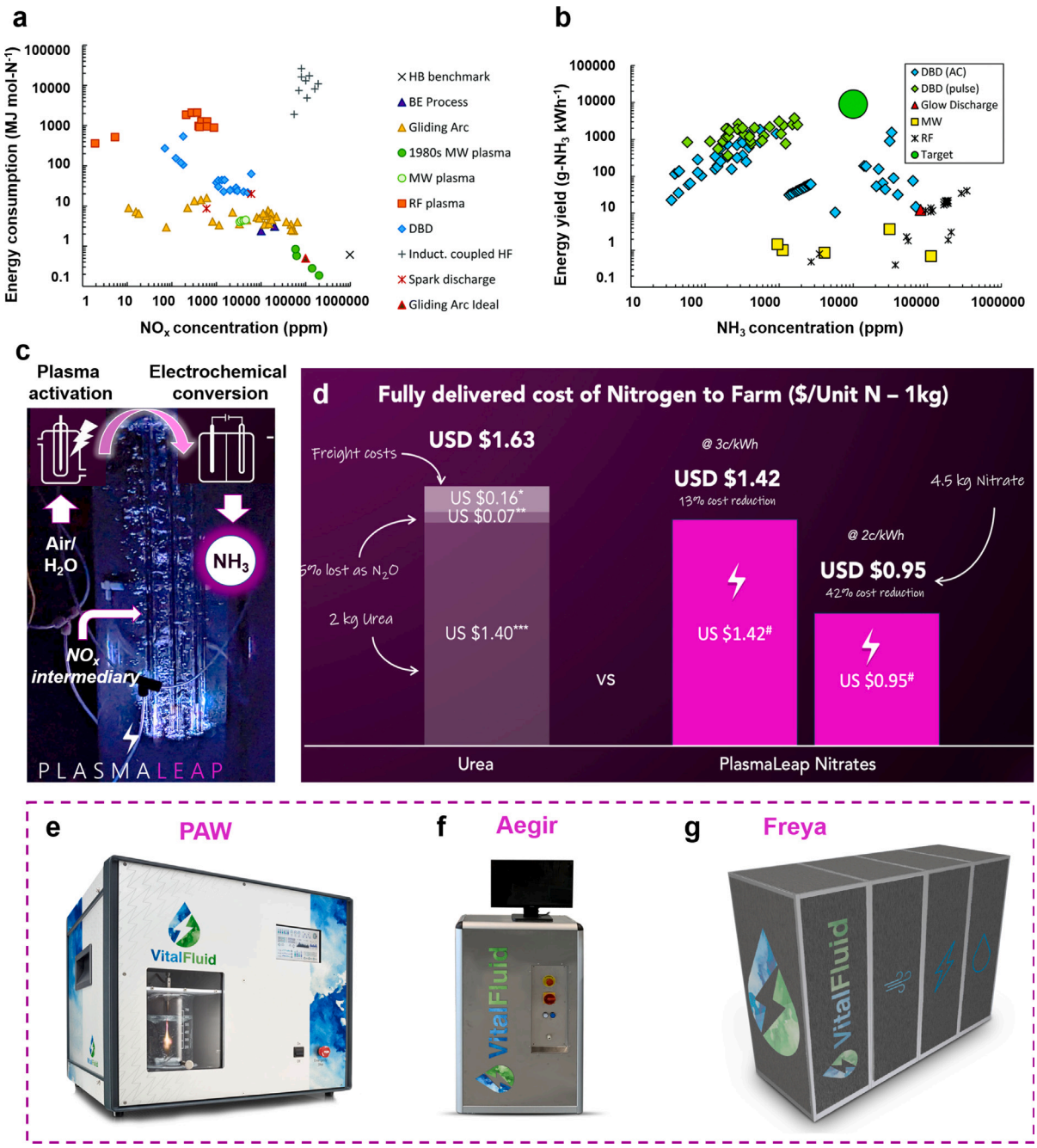

Fig. 9. (a) Energy consumption by various plasma-based reactors for NO_x production [25]. (b) Comparison of the energy yield of different plasma-assisted versus ammonia production concentration studies [16]. (c) Patented technology by PlasmaLeap Pty. Ltd. (Australia) for ammonia generation with zero-emissions and (d) Commercial viability of PlasmaLeap technology for nitrogen fixation and its comparison with traditional Urea fertilize [199]. Plasma activation units developed by VitalFluid (Netherlands) for many agriculture, medical and cleaning applications: (e) PAW at lab-scale level, (f) Aegir and (g) Freya [200].

result in a very low production of NH_3. For instance, an excess of 10% NH_3 yield consumed over 80 MJ per mol of (NH_3), while the process with low energy usage, 2 MJ per mol of NH_3 yielded a diluted NH_3 product (<0.1%) [113]. For the later, recovery of NH_3 from such a diluted mixture may require additional separation methods.

Recent investigation by Sun et al. using plasma-bubble coupled with electrocatalysis, the lowest energy consumption of was obtained as 3.2 ± 0.1 kWh mol^{-1} NH_4^+ (11.52 MJ) [155]. Another approach where a decentralized small-scale coupled plasma-catalytic was used for generating NO_x with subsequent trapping by lean NO_x trap (LNT) containing alkaline metal (Ba) led to an energy cost of 2.1 MJ mol^{-1}. Yet again, the energy requirement for a green H–B process running on water electrolysis is still lower (0.7 MJ mol^{-1} or 0.19 kWh mol^{-1}) [202]. The overall energy cost for NH_3 production via NO_x in plasma reactors using green H_2 is estimated to be in the range of 2.1 to 4.6 MJ mol^{-1} NH_3 [120,203]. The major reason for cost reduction is the activation of feed gas molecules at milder conditions without additional heating. In terms of nitrogen fixation for NO_x generation, the maximum energy efficiency achieved so far is 0.42 MJ (mol per N) [87]. However, the challenge here is the requirement of energy input for sustaining the stated process in Eq. (13) while 200 kJ mol^{-1} NO_x which is merely efficient (~4%) [195].

$$1/2N_{2(g)} + 5/4O_{2(g)} + 1/2H_2O_{(l)} \rightleftharpoons 2NO_{3(aq)}^- + H_{(aq)}^+ \quad (\Delta G = 7.3 \text{ kJ mol}^{-1} \text{ NO}_3^-) \tag{13}$$

There have been concerns about comparing the H–B process and plasma-assisted processes in terms of ammonia production. As already mentioned, the fully optimized H–B plant can produce ~2000 tons NH_3/day. However, miniaturization of the H–B process is not economically feasible due to thermodynamic limitations. Modification such as coupling with electrification using renewable energy has been suggested which is highly challenging. Nevertheless, such incorporation has to be done at a small scale, and even after that, the modified H–B process will be approximately two times more expensive than the conventional process [204,205]. Moreover, its operation cannot be matched to the fluctuations in renewable energy (such as solar and wind energy) production during the day.

Moreover, fertilizer production using the H–B process requires several energy-consuming steps. Since NH_3 is volatile, it is transformed into non-volatile ammonium nitrate (NH_4NO_3) through the Ostwald process which is later on used as fertilizer. For this purpose, NH_3 from H–B process is usually oxidized to produce NO_x (NO and NO_2) in a highly oxidized environment (Eqs. (14), (15)). Subsequently, HNO_3 is synthesized by NO_2 absorption in water (Eq. (16)). The as-formed nitric acid is then neutralized with NH_3 to NH_4NO_3 which in turn is used as fertilizer for agricultural purposes (Eq. (17)) [25].

$$4NH_3 + 5O_2 \rightarrow 4NO + 6H_2O \qquad (\Delta H_r^o = -905 \text{ kJ mol}^{-1}) \tag{14}$$

$$2NO + O_2 \rightarrow 2NO_2 \qquad (\Delta H_r^o = -114 \text{ kJ mol}^{-1}) \tag{15}$$

$$3NO_2 + H_2O \rightarrow 2HNO_3 + NO \qquad (\Delta H_r^o = -117 \text{ kJ mol}^{-1}) \tag{16}$$

$$NH_3 + HNO_3 \rightarrow NH_4NO_3 \tag{17}$$

Therefore, the overall process requires N_2 (N with oxidation state 0) which is firstly reduced to NH_3 (N with oxidation state −3), which is then oxidized again to NO (oxidation state +2). The conventional process requires H_2 as an energy source to drive this reaction. Consequently, synthesis of NH_4NO_3 fertilizer through the combination of H–B and Ostwald process is a detour process [81]. Notably, the Ostwald process consumes 66.6 GJ per ton of fixed nitrogen which is ~1.7 times the energy for NH_3 production [10]. Feeding the renewably produced H_2 through water splitting can reduce the CO_2, while the process adds huge energy input [206]. Thus, the process is energy-intensive and contradicts the current research focus on reducing energy consumption. Instead of this detour, a direct conversion of N_2 to NO_x presents a streamlined approach with the potential for enhanced efficiency.

Given all these complexities, the decentralized plasma-assisted technology-driven plants may act as a more suitable choice. Continuous development in catalyst activity permitting milder conditions and flexible plant designs are the few active research practices which further may provide a promising method for achieving cost-competitive green NH_3 generation. Access to intermittent renewable energy which may be enough to run small-scaled plasma-assisted NH_3 generators could be a game changer [120]. Such advantages make it compatible with localized, on-site ammonia production. Furthermore, small-scale plasma reactors can drastically eliminate the transportation cost. Therefore, it can contribute to sustainable ammonia generation for fertilizer applications. Moreover, fuel production storage can be carried on-site and complement the existing conventional processes [203].

The long-awaited target of decarbonized NH_3 synthesis, renewable (e.g., wind, solar energy, etc.) energy-driven cold plasmas for N_2 activation using water as a hydrogen source can be proposed (as shown in Fig. 1). One of the peculiar features is that air can be used as a source of N_2 for its conversion to nitrogen oxides (NO_x) which are usually first absorbed in water to form reactive NO_x^-. Co-existence of oxidative species, NO_x/NO_x^- may also lead to low yield and selectivity of ammonia synthesis, however, selection of plasma type, modulating catalyst design and adsorbent reaction medium coupled in electrocatalytic operation can enable selective conversion of NO_x^- to NH_3. Thus, the approach has a specific advantage over the other due to high efficiency and selectivity towards the NH_3 production. Moreover, the flexibility of tuning the catalysts, electrolyte, interface and potential may further enhance the selective generation of NH_3.

Anthropogenic nitrogenous harmful and toxic contaminants present in industrial wastewater and groundwater such as nitrate and nitrite (NO_x^-) can also be used as N source [207]. While it is also urgent to remediate the NO_x^- from wastewater for clean water availability, it can be used as a major source of N_2. Therefore, cold plasma accumulating high content of NO_x^- and its coupled electrochemical conversion to indispensable NH_3 are the focal point of research. Realizing the potential of pervasive contaminants, NO_2^- and NO_3^-, there have been attempts to use them for ammonia synthesis (as explained in Section 5.2). Alternatively, NO as feedstock in electrocatalytic approach has been suggested as the most efficient NO_x species for efficient and high selective production rates of ammonia [208]. This may be a turnaround for future research and can be marked as a key step in this field. Cold plasma technology for NO production is a promising sign providing additional motivation for using NO_x as a feedstock for ammonia synthesis [209]. Currently, such plasma catalytic approaches are in their infancy and require more efforts to be economically competitive.

Inspired by a two-stage pathway, the Plasmaleap (Australia) research group has developed a pilot plant system that is forecast to be commercially competitive with traditional fertilizer production (Fig. 9c) [199]. The pilot plant system uses a plasma-bubble reactor design powered by renewable electricity wherein atmospheric air and water were used N_2 and H_2 source respectively, to synthesize nitrate & ammonia derivatives. The pilot units were capable of deployment on a farm or in an industrial setting, which may completely remove transport and supply chain costs. Techno-economic evaluation of PlasmaLeap pilot plant for nitrate fertilizer revealed the production cost ranges from US$ 0.95 to US$ 1.42 in comparison to Urea, suggesting the commercial viability which can meet the future global fertilizer demand (Fig. 9d).

Similarly, VitalFluid, a Dutch company, fabricates a portable device to fix natural nitrogen applicable for seed treatment, natural plant protection, and cleaning applications [200]. Lab-scale unit, PAW producing 0.5 L activated water per batch is available for feasibility and proof of concept testing for disinfecting applications with plasma water (Fig. 9e). For higher capacity, "Aegir" is developed which is operated at 1 kW power that generates instant 2 L of plasma activated water per batch (Fig. 9f). Another device, "Freya", works on high power (15 kW) for scalable PAW production at the rate of 9.5 mol NO_3^- per hour (0.6 kg) which can be maximized up to 300 mmol NO_3^- per liter concentration (Fig. 9g). The Freya is suitable for 24/7 operation and can be used for hydroponic growers, vertical farming and fertigation. These innovations are successful examples of the implementation of cold plasma technology contributing towards sustainable production of nitrogen nutrients and agrochemicals.

7. Summary and outlook: Propositions for cold plasma catalyzed green NH_3 synthesis for sustainability

A plethora of research is available in the field of plasma-based nitrogen fixation for NO_x or direct NH_3 synthesis. Reaction pathways for N_2 fixation under plasma conditions need to be improved to match the efficiency of the benchmark H–B process. Currently, the energy consumption for plasma-assisted conversion of N_2/H_2 into NH_3 seems to vary wherein reported values ranged from several 100 MJ/mol to the order of 1 MJ/mol [148]. Synthesis of ammonia via plasma-assisted two-stage pathway of $N_2 \rightarrow NO_x \rightarrow NH_3$ process requires consideration both of N_2 oxidation to NO_x and NO_x transformation to NH_3 wherein viability of large-scale production in former step is less unknown.

In terms of fertilizer production, the conventional process is a detour that requires breaking of the synthesized NH_3 to form NH_3NO_3 (Eqs. (14)–(17)). Cold plasma-assisted NO_x^- production simplifies and

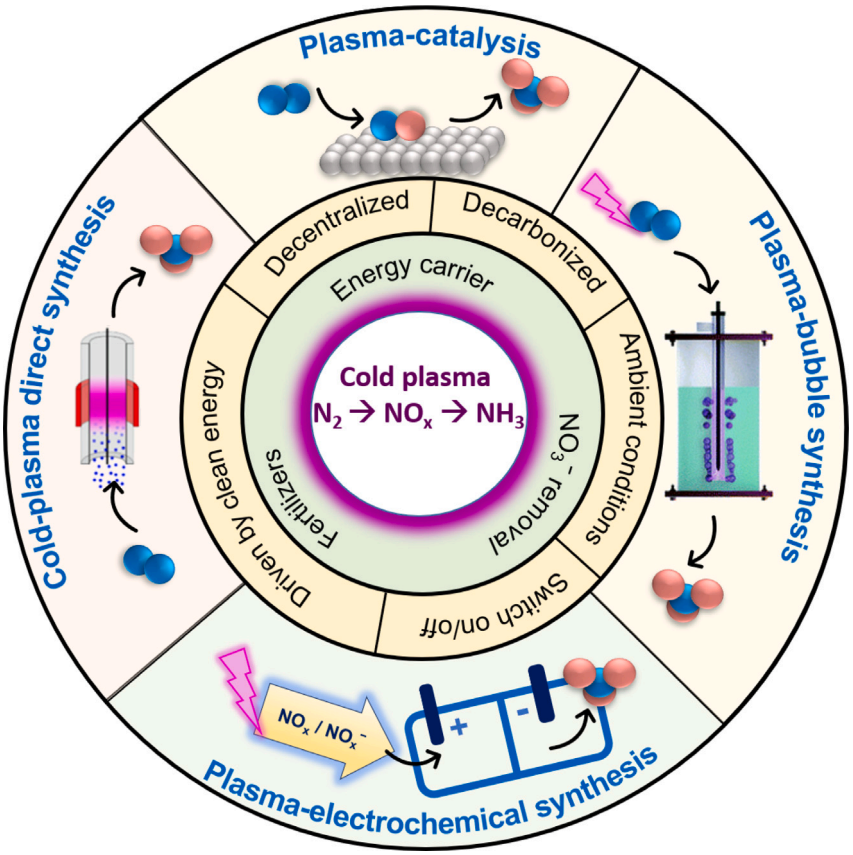

Fig. 10. Role of cold plasma-assisted technology in energy and environmental remediation as shown by green colored co-centric ring. Two-stage pathway not only can use NO_3^- as reactant but also can be potentially transformed into NH_3. The yellow ring indicates the various advantages of cold plasma technology suitable for sustainable NH_3 production. The last ring shows major plasma-assisted technologies to achieve ammonia synthesis.

reduces these additional energy-intensive steps. Furthermore, cold plasma exhibits multiple advantageous attributes including its operation under milder conditions (ambient conditions of temperature and pressure), easily switched on/off and, and its amenability to being powered by renewable electricity sources to produce NH_3 serving both as an energy carrier and a fertilizer precursor. Cold plasma-assisted technology offers decentralized on-site ammonia production addressing the pollution associated with the storage, transportation and distribution of fertilizer to localized farmers. Establishing the network of small-scale renewable energy to power cold plasma-assisted reactors, on-site NH_3 production cuts down not only the distribution costs but also reduces our dependency on fossil fuels.

Fig. 10 showcases the unequivocal benefits of cold-plasma assisted technology for the sustainable production and application of ammonia and its derivatives for energy and environmental applications (green ring). The yellow ring of the figure pinpoints the feasibility of cold plasma-assisted technology, while the largest one shows the major technology for achieving NH_3 production. The techno-economic status is subject to the inevitable uncertainties of early-stage technologies. Nevertheless, the reports indicating advanced and selective NO_x formation in the recent literature are a promising sign [208,209].

Cold plasma coupled with bubble technology maximizing reactive NO_x species at gas-liquid interface via intensifying gas-to-liquid mass transfer of afterglow reactive species is another active research horizon that may be explored for large-scale production of NO_x [155,175,178,210]. The increased interfacial areas, elevated internal pressure and subsequent bursting, deliver the reactive species on-site for their enhanced action.

Several specific research directions need to be explored such as (i) design and synthesis of effective catalysts for the plasma conversion and for selectivity of active species; (ii) understanding and controlling of flow dynamics of gas phase and the liquid in cold plasma (micro) discharge to achieve optimal energy efficiency, (iii) maximize the synergy of long and short lived active species; and (iv) rational device design integrated with the discharge powered by renewable energy achieving stable operations for sustainable ammonia generation. Real-time diagnosis for monitoring the plasma-catalysis system is imperative to understand these questions and elucidate reaction pathways for improving the functionalities of plasma-catalysis synergism. Combining all the key factors may lead to a robust system, wherein plasma-based technology driven by renewable energy sources will become suitable for sustainable NH_3 production.

The cold plasma-assisted ammonia synthesis involves multi-phase and multi-scale reaction processes, exchange of mass and energy, plasma-physics, materials discovery, and device engineering. Forging an envision of cold plasma-assisted technology for sustainable ammonia production for energy fuel and agricultural purposes will require joint efforts from multi-disciplinary scientific communities worldwide. In this endeavor, artificial intelligence (AI) may aid the research on this complicated process due to its ability to handle multidimensional problems. AI may help accelerate the processes of catalyst discovery, identifying the reaction conditions for selectivity and optimization of energy efficiency.

CRediT authorship contribution statement

Deepak Panchal: Writing – review & editing, Writing – original draft, Visualization, Investigation, Data curation, Conceptualization. **Qiuyun Lu:** Writing – original draft, Methodology, Investigation, Formal analysis. **Ken Sakaushi:** Visualization, Supervision, Formal analysis. **Xuehua Zhang:** Writing – review & editing, Supervision, Resources, Project administration, Funding acquisition, Conceptualization.

Declaration of competing interest

The authors declare that they have no known competing financial interests or personal relationships that could have appeared to influence the work reported in this paper.

Data availability

No data was used for the research described in the article.

Acknowledgments

This project is supported by the Alberta Innovates, Canada. This work was undertaken, in part, thanks to funding from the Canada Research Chairs Program.

References

[1] A. Bogaerts, E.C. Neyts, Plasma technology: an emerging technology for energy storage, ACS Energy Lett. 3 (4) (2018) 1013–1027.
[2] B.K. Sovacool, P. Schmid, A. Stirling, G. Walter, G. MacKerron, Differences in carbon emissions reduction between countries pursuing renewable electricity versus nuclear power, Nat. Energy 5 (11) (2020) 928–935.
[3] S.Z. Al Ghafri, S. Munro, U. Cardella, T. Funke, W. Notardonato, J.M. Trusler, J. Leachman, R. Span, S. Kamiya, G. Pearce, et al., Hydrogen liquefaction: a review of the fundamental physics, engineering practice and future opportunities, Energy Environ. Sci. 15 (7) (2022) 2690–2731.
[4] F. Chang, W. Gao, J. Guo, P. Chen, Emerging materials and methods toward ammonia-based energy storage and conversion, Adv. Mater. 33 (50) (2021) 2005721.
[5] S. Ristig, M. Poschmann, J. Folke, O. Gómez-Cápiro, Z. Chen, N. Sanchez-Bastardo, R. Schlögl, S. Heumann, H. Ruland, Ammonia decomposition in the process chain for a renewable hydrogen supply, Chem. Ing. Tech. 94 (10) (2022) 1413–1425.
[6] L. Zhou, X. Li, Q. Li, A. Kalu, C. Liu, X. Liu, W. Li, Advances in nitrogen carriers for chemical looping processes for sustainable and carbon-free ammonia synthesis, ACS Catal. 13 (22) (2023) 15087–15106.
[7] A. Valera-Medina, F. Amer-Hatem, A.K. Azad, I. Dedoussi, M. De Joannon, R. Fernandes, P. Glarborg, H. Hashemi, X. He, S. Mashruk, et al., Review on ammonia as a potential fuel: from synthesis to economics, Energy Fuels 35 (9) (2021) 6964–7029.
[8] K.H. Rouwenhorst, S. Mani, L. Lefferts, Improving the energy yield of plasma-based ammonia synthesis with in situ adsorption, ACS Sustain. Chem. Eng. 10 (6) (2022) 1994–2000.
[9] M.J. Palys, P. Daoutidis, Optimizing renewable ammonia production for a sustainable fertilizer supply chain transition, ChemSusChem 16 (22) (2023) e202300563.
[10] J. Lim, C.A. Fernández, S.W. Lee, M.C. Hatzell, Ammonia and nitric acid demands for fertilizer use in 2050, ACS Energy Lett. 6 (10) (2021) 3676–3685.
[11] A. Klerke, C.H. Christensen, J.K. Nørskov, T. Vegge, Ammonia for hydrogen storage: challenges and opportunities, J. Mater. Chem. 18 (20) (2008) 2304–2310.
[12] M.A. Nawaz, R. Blay-Roger, M. Saif, F. Meng, J. González-Arias, B. Miao, L.F. Bobadilla, T. Ramirez-Reina, J. Odriozola, Enroute to the carbon-neutrality goals via the targeted development of ammonia as a potential nitrogen-based energy carrier, ACS Catal. 13 (21) (2023) 14415–14453.
[13] D.R. MacFarlane, P.V. Cherepanov, J. Choi, B.H. Suryanto, R.Y. Hodgetts, J.M. Bakker, F.M.F. Vallana, A.N. Simonov, A roadmap to the ammonia economy, Joule 4 (6) (2020) 1186–1205.
[14] L. Torrente-Murciano, C. Smith, Process challenges of green ammonia production, Nat. Synth. 2 (7) (2023) 587–588.
[15] J.R. Jennings, Catalytic Ammonia Synthesis: Fundamentals and Practice, Springer Science & Business Media, 1991.
[16] K.H. Rouwenhorst, Y. Engelmann, K. van't Veer, R.S. Postma, A. Bogaerts, L. Lefferts, Plasma-driven catalysis: green ammonia synthesis with intermittent electricity, Green Chem. 22 (19) (2020) 6258–6287.
[17] D. Zhou, R. Zhou, R. Zhou, B. Liu, T. Zhang, Y. Xian, P.J. Cullen, X. Lu, K.K. Ostrikov, Sustainable ammonia production by non-thermal plasmas: Status, mechanisms, and opportunities, Chem. Eng. J. 421 (2021) 129544.
[18] I. Tsonev, C. O'Modhrain, A. Bogaerts, Y. Gorbanev, Nitrogen fixation by an arc plasma at elevated pressure to increase the energy efficiency and production rate of NOx, ACS Sustain. Chem. Eng. 11 (5) (2023) 1888–1897.
[19] T. Ding, M. Wang, F. Wu, B. Song, K. Lu, H. Zhang, Recent advances in electrocatalytic nitrate reduction: Strategies to promote ammonia synthesis, ACS Appl. Energy Mater. (2024).
[20] J. Wang, T. Feng, J. Chen, V. Ramalingam, Z. Li, D.M. Kabtamu, J.-H. He, X. Fang, Electrocatalytic nitrate/nitrite reduction to ammonia synthesis using metal nanocatalysts and bio-inspired metalloenzymes, Nano Energy 86 (2021) 106088.
[21] R.K. Sharma, H. Patel, U. Mushtaq, V. Kyriakou, G. Zafeiropoulos, F. Peeters, S. Welzel, M.C. Van De Sanden, M.N. Tsampas, Plasma activated electrochemical ammonia synthesis from nitrogen and water, ACS Energy Lett. 6 (2) (2020) 313–319.
[22] E.C. Neyts, K. Ostrikov, M.K. Sunkara, A. Bogaerts, Plasma catalysis: synergistic effects at the nanoscale, Chem. Rev. 115 (24) (2015) 13408–13446.
[23] J. Hong, S. Prawer, A.B. Murphy, Plasma catalysis as an alternative route for ammonia production: status, mechanisms, and prospects for progress, ACS Sustain. Chem. Eng. 6 (1) (2018) 15–31.
[24] J. Zhang, X. Li, J. Zheng, M. Du, X. Wu, J. Song, C. Cheng, T. Li, W. Yang, Non-thermal plasma-assisted ammonia production: A review, Energy Convers. Manage. 293 (2023) 117482.
[25] K.H. Rouwenhorst, F. Jardali, A. Bogaerts, L. Lefferts, From the birkeland–eyde process towards energy-efficient plasma-based NO x synthesis: a techno-economic analysis, Energy Environ. Sci. 14 (5) (2021) 2520–2534.
[26] Z. Qu, R. Zhou, J. Sun, Y. Gao, Z. Li, T. Zhang, R. Zhou, D. Liu, X. Tu, P. Cullen, et al., Plasma-assisted sustainable nitrogen-to-ammonia fixation: Mixed-phase, synergistic processes and mechanisms, ChemSusChem (2023) e202300783.
[27] N. Cherkasov, A. Ibhadon, P. Fitzpatrick, A review of the existing and alternative methods for greener nitrogen fixation, Chem. Eng. Process.: Process Intensif. 90 (2015) 24–33.
[28] O. Lemmermann, Alwin mittasch: Geschichte der ammoniaksynthese. Verlag chemie, Berlin-Weinheim, 1951. 196 seiten mit 12 bildtafeln und 4 abbildungen. ganzleinen DM 13, 20, 1951.
[29] H. Iriawan, S.Z. Andersen, X. Zhang, B.M. Comer, J. Barrio, P. Chen, A.J. Medford, I.E. Stephens, I. Chorkendorff, Y. Shao-Horn, Methods for nitrogen activation by reduction and oxidation, Nat. Rev. Methods Prim. 1 (1) (2021) 56.
[30] K. Lee, X. Liu, P. Vyawahare, P. Sun, A. Elgowainy, M. Wang, Techno-economic performances and life cycle greenhouse gas emissions of various ammonia production pathways including conventional, carbon-capturing, nuclear-powered, and renewable production, Green Chem. 24 (12) (2022) 4830–4844.
[31] H.-H. Kim, Y. Teramoto, A. Ogata, H. Takagi, T. Nanba, Plasma catalysis for environmental treatment and energy applications, Plasma Chem. Plasma Process. 36 (2016) 45–72.
[32] H.-P. Jia, E.A. Quadrelli, Mechanistic aspects of dinitrogen cleavage and hydrogenation to produce ammonia in catalysis and organometallic chemistry: relevance of metal hydride bonds and dihydrogen, Chem. Soc. Rev. 43 (2) (2014) 547–564.
[33] W. Gao, J. Guo, P. Wang, Q. Wang, F. Chang, Q. Pei, W. Zhang, L. Liu, P. Chen, Production of ammonia via a chemical looping process based on metal imides as nitrogen carriers, Nat. Energy 3 (12) (2018) 1067–1075.
[34] J. Sun, D. Alam, R. Daiyan, H. Masood, T. Zhang, R. Zhou, P.J. Cullen, E.C. Lovell, A.R. Jalili, R. Amal, A hybrid plasma electrocatalytic process for sustainable ammonia production, Energy Environ. Sci. 14 (2) (2021) 865–872.
[35] X. Fu, J.B. Pedersen, Y. Zhou, M. Saccoccio, S. Li, R. Sažinas, K. Li, S.Z. Andersen, A. Xu, N.H. Deissler, et al., Continuous-flow electrosynthesis of ammonia by nitrogen reduction and hydrogen oxidation, Science 379 (6633) (2023) 707–712.
[36] D.F. Swearer, N.R. Knowles, H.O. Everitt, N.J. Halas, Light-driven chemical looping for ammonia synthesis, ACS Energy Lett. 4 (7) (2019) 1505–1512.
[37] A. Tsuneto, A. Kudo, T. Sakata, Efficient electrochemical reduction of N2 to NH3 catalyzed by lithium, Chem. Lett. (5) (1993) 851–854.
[38] A. Liu, Y. Yang, X. Ren, Q. Zhao, M. Gao, W. Guan, F. Meng, L. Gao, Q. Yang, X. Liang, et al., Current progress of electrocatalysts for ammonia synthesis through electrochemical nitrogen reduction under ambient conditions, ChemSusChem 13 (15) (2020) 3766–3788.
[39] B. Yang, W. Ding, H. Zhang, S. Zhang, Recent progress in electrochemical synthesis of ammonia from nitrogen: strategies to improve the catalytic activity and selectivity, Energy Environ. Sci. 14 (2) (2021) 672–687.
[40] F. Zhou, L.M. Azofra, M. Ali, M. Kar, A.N. Simonov, C. McDonnell-Worth, C. Sun, X. Zhang, D.R. MacFarlane, Electro-synthesis of ammonia from nitrogen at ambient temperature and pressure in ionic liquids, Energy Environ. Sci. 10 (12) (2017) 2516–2520.
[41] U.K. Ghorai, S. Paul, B. Ghorai, A. Adalder, S. Kapse, R. Thapa, A. Nagendra, A. Gain, Scalable production of cobalt phthalocyanine nanotubes: efficient and robust hollow electrocatalyst for ammonia synthesis at room temperature, ACS Nano 15 (3) (2021) 5230–5239.
[42] H.-L. Du, M. Chatti, R.Y. Hodgetts, P.V. Cherepanov, C.K. Nguyen, K. Matuszek, D.R. MacFarlane, A.N. Simonov, Electroreduction of nitrogen with almost 100% current-to-ammonia efficiency, Nature 609 (7928) (2022) 722–727.
[43] B.H. Suryanto, H.-L. Du, D. Wang, J. Chen, A.N. Simonov, D.R. MacFarlane, Challenges and prospects in the catalysis of electroreduction of nitrogen to ammonia, Nat. Catal. 2 (4) (2019) 290–296.

[44] Y. Luo, H. Jiang, L.-X. Ding, S. Chen, Y. Zou, G.-F. Chen, H. Wang, Selective synthesis of either nitric acid or ammonia from air by electrolyte regulation in a plasma electrolytic system, ACS Sustain. Chem. Eng. 11 (32) (2023) 11737–11744.
[45] S. Li, Y. Zhou, K. Li, M. Saccoccio, R. Sažinas, S.Z. Andersen, J.B. Pedersen, X. Fu, V. Shadravan, D. Chakraborty, et al., Electrosynthesis of ammonia with high selectivity and high rates via engineering of the solid-electrolyte interphase, Joule 6 (9) (2022) 2083–2101.
[46] N. Lazouski, A. Limaye, A. Bose, M.L. Gala, K. Manthiram, D.S. Mallapragada, Cost and performance targets for fully electrochemical ammonia production under flexible operation, ACS Energy Lett. 7 (8) (2022) 2627–2633.
[47] W. Gao, P. Wang, J. Guo, F. Chang, T. He, Q. Wang, G. Wu, P. Chen, Barium hydride-mediated nitrogen transfer and hydrogenation for ammonia synthesis: a case study of cobalt, ACS Catal. 7 (5) (2017) 3654–3661.
[48] J. Guo, P. Chen, Interplay of alkali, transition metals, nitrogen, and hydrogen in ammonia synthesis and decomposition reactions, Acc. Chem. Res. 54 (10) (2021) 2434–2444.
[49] Z. Li, Y. Lu, J. Li, M. Xu, Y. Qi, S.-W. Park, M. Kitano, H. Hosono, J.-S. Chen, T.-N. Ye, Multiple reaction pathway on alkaline earth imide supported catalysts for efficient ammonia synthesis, Nature Commun. 14 (1) (2023) 6373.
[50] P. Wang, F. Chang, W. Gao, J. Guo, G. Wu, T. He, P. Chen, Breaking scaling relations to achieve low-temperature ammonia synthesis through LiH-mediated nitrogen transfer and hydrogenation, Nat. Chem. 9 (1) (2017) 64–70.
[51] Q. Wang, J. Guo, P. Chen, The impact of alkali and alkaline earth metals on green ammonia synthesis, Chem 7 (12) (2021) 3203–3220.
[52] J.A. Schwalbe, M.J. Statt, C. Chosy, A.R. Singh, B.A. Rohr, A.C. Nielander, S.Z. Andersen, J.M. McEnaney, J.G. Baker, T.F. Jaramillo, et al., A combined theory-experiment analysis of the surface species in lithium-mediated NH3 electrosynthesis, ChemElectroChem 7 (7) (2020) 1542–1549.
[53] K. Li, S.Z. Andersen, M.J. Statt, M. Saccoccio, V.J. Bukas, K. Krempl, R. Sažinas, J.B. Pedersen, V. Shadravan, Y. Zhou, et al., Enhancement of lithium-mediated ammonia synthesis by addition of oxygen, Science 374 (6575) (2021) 1593–1597.
[54] W. Chang, A. Jain, F. Rezaie, K. Manthiram, Lithium-mediated nitrogen reduction to ammonia via the catalytic solid–electrolyte interphase, Nat. Catal. (2024) 1–11.
[55] S.Z. Andersen, V. Čolić, S. Yang, J.A. Schwalbe, A.C. Nielander, J.M. McEnaney, K. Enemark-Rasmussen, J.G. Baker, A.R. Singh, B.A. Rohr, et al., A rigorous electrochemical ammonia synthesis protocol with quantitative isotope measurements, Nature 570 (7762) (2019) 504–508.
[56] R. Lan, J.T. Irvine, S. Tao, Synthesis of ammonia directly from air and water at ambient temperature and pressure, Sci. Rep. 3 (1) (2013) 1145.
[57] M.-M. Shi, D. Bao, B.-R. Wulan, Y.-H. Li, Y.-F. Zhang, J.-M. Yan, Q. Jiang, Au sub-nanoclusters on TiO2 toward highly efficient and selective electrocatalyst for N2 conversion to NH3 at ambient conditions, Adv. Mater. 29 (17) (2017) 1606550.
[58] L.F. Greenlee, J.N. Renner, S.L. Foster, The use of controls for consistent and accurate measurements of electrocatalytic ammonia synthesis from dinitrogen, ACS Catal. 8 (9) (2018) 7820–7827.
[59] S. Xu, H. Chen, X. Fan, Rational design of catalysts for non-thermal plasma (NTP) catalysis: A reflective review, Catal. Today (2023) 114144.
[60] T. Zhang, R. Zhou, S. Zhang, R. Zhou, J. Ding, F. Li, J. Hong, L. Dou, T. Shao, A.B. Murphy, et al., Sustainable ammonia synthesis from nitrogen and water by one-step plasma catalysis, Energy Environ. Mater. 6 (2) (2023) e12344.
[61] C. Ndayirinde, Y. Gorbanev, R.-G. Ciocarlan, R. De Meyer, A. Smets, E. Vlasov, S. Bals, P. Cool, A. Bogaerts, Plasma-catalytic ammonia synthesis: Packed catalysts act as plasma modifiers, Catal. Today 419 (2023) 114156.
[62] Z. Huang, A. Xiao, D. Liu, X. Lu, K. Ostrikov, Plasma-water-based nitrogen fixation: Status, mechanisms, and opportunities, Plasma Process. Polym. 19 (4) (2022) 2100198.
[63] X. Zeng, S. Zhang, Y. Liu, X. Hu, K.K. Ostrikov, T. Shao, Energy-efficient pathways for pulsed-plasma-activated sustainable ammonia synthesis, ACS Sustain. Chem. Eng. 11 (3) (2023) 1110–1120.
[64] A.K. Brewer, J. Westhaver, The synthesis of ammonia in the glow discharge, J. Phys. Chem. 33 (6) (2002) 883–895.
[65] H. Uyama, O. Matsumoto, Synthesis of ammonia in high-frequency discharges. II. Synthesis of ammonia in a microwave discharge under various conditions, Plasma Chem. Plasma Process. 9 (1989) 421–432.
[66] P. Navascués, J.M. Obrero-Pérez, J. Cotrino, A.R. González-Elipe, A. Gómez-Ramírez, Unraveling discharge and surface mechanisms in plasma-assisted ammonia reactions, ACS Sustain. Chem. Eng. 8 (39) (2020) 14855–14866.
[67] V.S. Gharahshiran, Y. Zheng, Sustainable ammonia synthesis: An in-depth review of non-thermal plasma technologies, J. Energy Chem. (2024).
[68] M. Kim, S. Biswas, G. Nava, B.M. Wong, L. Mangolini, Reduced energy cost of ammonia synthesis via RF plasma pulsing, ACS Sustain. Chem. Eng. 10 (46) (2022) 15135–15147.
[69] J. Li, Q. Xiong, X. Mu, L. Li, Recent advances in ammonia synthesis: From haber-bosch process to external field driven strategies, ChemSusChem (2024) e202301775.
[70] K. Kyere-Yeboah, I.K. Bique, X.-c. Qiao, Advances of non-thermal plasma discharge technology in degrading recalcitrant wastewater pollutants. A comprehensive review, Chemosphere 320 (2023) 138061.
[71] A. Hassan, S. Abd El Aal, M. Shehata, A. El-Saftawy, Plasma-etching and modification of polyethylene for improved surface structure, wettability and optical behavior, Surf. Rev. Lett. 26 (07) (2019) 1850220.
[72] V.M. Shmelev, A.V. Saveliev, L.A. Kennedy, Plasma chemical reactor with exploding water jet, Plasma Chem. Plasma Process. 29 (2009) 275–290.
[73] B. Patil, N. Cherkasov, J. Lang, A. Ibhadon, V. Hessel, Q. Wang, Low temperature plasma-catalytic NOx synthesis in a packed DBD reactor: Effect of support materials and supported active metal oxides, Appl. Catal. B 194 (2016) 123–133.
[74] B. Patil, J. Rovira Palau, V. Hessel, J. Lang, Q. Wang, Plasma nitrogen oxides synthesis in a milli-scale gliding arc reactor: investigating the electrical and process parameters, Plasma Chem. Plasma Process. 36 (2016) 241–257.
[75] M. Janda, V. Martišovitš, K. Hensel, Z. Machala, Generation of antimicrobial NO x by atmospheric air transient spark discharge, Plasma Chem. Plasma Process. 36 (2016) 767–781.
[76] M.A. Malik, C. Jiang, R. Heller, J. Lane, D. Hughes, K.H. Schoenbach, Ozone-free nitric oxide production using an atmospheric pressure surface discharge–a way to minimize nitrogen dioxide co-production, Chem. Eng. J. 283 (2016) 631–638.
[77] X. Pei, D. Gidon, Y.-J. Yang, Z. Xiong, D.B. Graves, Reducing energy cost of NOx production in air plasmas, Chem. Eng. J. 362 (2019) 217–228.
[78] F. Jardali, S. Van Alphen, J. Creel, H.A. Eshtehardi, M. Axelsson, R. Ingels, R. Snyders, A. Bogaerts, NO x production in a rotating gliding arc plasma: Potential avenue for sustainable nitrogen fixation, Green Chem. 23 (4) (2021) 1748–1757.
[79] E. Vervloessem, M. Aghaei, F. Jardali, N. Hafezkhiabani, A. Bogaerts, Plasma-based n2 fixation into no x: insights from modeling toward optimum yields and energy costs in a gliding arc plasmatron, ACS Sustain. Chem. Eng. 8 (26) (2020) 9711–9720.
[80] L. Li, C. Tang, X. Cui, Y. Zheng, X. Wang, H. Xu, S. Zhang, T. Shao, K. Davey, S.-Z. Qiao, Efficient nitrogen fixation to ammonia through integration of plasma oxidation with electrocatalytic reduction, Angew. Chem. 133 (25) (2021) 14250–14256.
[81] J. Ding, W. Li, Q. Chen, J. Liu, S. Tang, Z. Wang, L. Chen, H. Zhang, Sustainable ammonia synthesis from air by the integration of plasma and electrocatalysis techniques, Inorg. Chem. Front. 10 (19) (2023) 5762–5771.
[82] X. Pei, Y. Li, Y. Luo, C. Man, Y. Zhang, X. Lu, D.B. Graves, Nitrogen fixation as NOx using air plasma coupled with heterogeneous catalysis at atmospheric pressure, Plasma Process. Polym. 21 (1) (2024) 2300135.
[83] P. Lamichhane, N. Pourali, E.V. Rebrov, V. Hessel, Sustainable plasma-catalytic nitrogen fixation with pyramid shaped μ-electrode DBD and titanium dioxide, ChemistrySelect 9 (24) (2024) e202401076.
[84] A.A. Abdelaziz, Y. Teramoto, T. Nozaki, H.-H. Kim, Toward reducing the energy cost of NO x formation in a spark discharge reactor through pinpointing its mechanism, ACS Sustain. Chem. Eng. 11 (10) (2023) 4106–4118.
[85] J. Li, C. Lan, L. Nie, D. Liu, X. Lu, Distributed plasma-water-based nitrogen fixation system based on cascade discharge: Generation, regulation, and application, Chem. Eng. J. 478 (2023) 147483.
[86] A.A. Abdelaziz, Y. Teramoto, T. Nozaki, H.-H. Kim, Performance of high-frequency spark discharge for efficient NOx production with tunable selectivity, Chem. Eng. J. 470 (2023) 144182.
[87] E. Vervloessem, Y. Gorbanev, A. Nikiforov, N. De Geyter, A. Bogaerts, Sustainable NO x production from air in pulsed plasma: elucidating the chemistry behind the low energy consumption, Green Chem. 24 (2) (2022) 916–929.
[88] W. Wang, B. Patil, S. Heijkers, V. Hessel, A. Bogaerts, Nitrogen fixation by gliding arc plasma: better insight by chemical kinetics modelling, ChemSusChem 10 (10) (2017) 2145–2157.
[89] M. Majeed, M. Iqbal, M. Altin, Y.-N. Kim, D.K. Dinh, C. Lee, Z. Ali, D.H. Lee, Effect of thermal gas quenching on NOx production by atmospheric pressure rotating arc plasma: a pathway towards eco-friendly fertilizer, Chem. Eng. J. 485 (2024) 149727.
[90] Q. Wang, L. Liu, G. Gao, Y. Chen, Y. Ouyang, D. Zhang, Y. Su, S. Ding, Insights on the mechanism of surface-catalyzed oxidative nitrogen fixation based on liquid-phase bubble pin-plate discharge, ACS Catal. 14 (7) (2024) 4719–4727.
[91] Y. Zhang, C. Zhu, H. Wei, Y. Tian, W. Xia, C. Wang, A highly effective N2 fixation method based on reverse vortex flow gliding arc plasma under water, J. Clean. Prod. 452 (2024) 142158.
[92] S. Deng, W. Xing, T. Sato, S. Zen, N. Takeuchi, Experimental and theoretical study on reactive oxygen and nitrogen species generation in plasma bubbles with ammonia solution, Plasma Process. Polym. (2024) e2300223.
[93] T.-Q. Zhang, X.-S. Li, J.-L. Liu, X.-Q. Wen, A.-M. Zhu, Plasma nitrogen fixation: NOx synthesis in MnOx/Al2O3 packed-bed dielectric barrier discharge, Plasma Chem. Plasma Process. 43 (6) (2023) 1907–1919.
[94] S. Kelly, A. Bogaerts, Nitrogen fixation in an electrode-free microwave plasma, Joule 5 (11) (2021) 3006–3030.

[95] P. Peng, P. Chen, M. Addy, Y. Cheng, E. Anderson, N. Zhou, C. Schiappacasse, Y. Zhang, D. Chen, R. Hatzenbeller, et al., Atmospheric plasma-assisted ammonia synthesis enhanced via synergistic catalytic absorption, ACS Sustain. Chem. Eng. 7 (1) (2018) 100–104.
[96] U. Kogelschatz, Dielectric-barrier discharges: their history, discharge physics, and industrial applications, Plasma Chem. Plasma Process. 23 (1) (2003) 1–46.
[97] N.C. Roy, N. Maira, C. Pattyn, A. Remy, M.-P. Delplancke, F. Reniers, Mechanisms of reducing energy costs for nitrogen fixation using air-based atmospheric DBD plasmas over water in contact with the electrode, Chem. Eng. J. 461 (2023) 141844.
[98] J. Jose, S. Ramanujam, L. Philip, Applicability of pulsed corona discharge treatment for the degradation of chloroform, Chem. Eng. J. 360 (2019) 1341–1354.
[99] Y. Miao, A. Yokochi, G. Jovanovic, S. Zhang, A. von Jouanne, Application-oriented non-thermal plasma in chemical reaction engineering: A review, Green Energy Resour. 1 (1) (2023) 100004.
[100] S. Van Alphen, H.A. Eshtehardi, C. O'Modhrain, J. Bogaerts, H. Van Poyer, J. Creel, M.-P. Delplancke, R. Snyders, A. Bogaerts, Effusion nozzle for energy-efficient NOx production in a rotating gliding arc plasma reactor, Chem. Eng. J. 443 (2022) 136529.
[101] X. Bai, S. Tiwari, B. Robinson, C. Killmer, L. Li, J. Hu, Microwave catalytic synthesis of ammonia from methane and nitrogen, Catal. Sci. Technol. 8 (24) (2018) 6302–6305.
[102] J. Shah, W. Wang, A. Bogaerts, M.L. Carreon, Ammonia synthesis by radio frequency plasma catalysis: revealing the underlying mechanisms, ACS Appl. Energy Mater. 1 (9) (2018) 4824–4839.
[103] J. Humphreys, R. Lan, S. Tao, Development and recent progress on ammonia synthesis catalysts for Haber–Bosch process, Adv. Energy Sustain. Res. 2 (1) (2021) 2000043.
[104] J. Hong, S. Prawer, A.B. Murphy, Production of ammonia by heterogeneous catalysis in a packed-bed dielectric-barrier discharge: influence of argon addition and voltage, IEEE Trans. Plasma Sci. 42 (10) (2014) 2338–2339.
[105] J. Hong, M. Aramesh, O. Shimoni, D.H. Seo, S. Yick, A. Greig, C. Charles, S. Prawer, A.B. Murphy, Plasma catalytic synthesis of ammonia using functionalized-carbon coatings in an atmospheric-pressure non-equilibrium discharge, Plasma Chem. Plasma Process. 36 (2016) 917–940.
[106] P. Peng, Y. Li, Y. Cheng, S. Deng, P. Chen, R. Ruan, Atmospheric pressure ammonia synthesis using non-thermal plasma assisted catalysis, Plasma Chem. Plasma Process. 36 (2016) 1201–1210.
[107] M. Iwamoto, M. Akiyama, K. Aihara, T. Deguchi, Ammonia synthesis on wool-like Au, Pt, Pd, Ag, or Cu electrode catalysts in nonthermal atmospheric-pressure plasma of N2 and H2, ACS Catal. 7 (10) (2017) 6924–6929.
[108] Y. Wang, M. Craven, X. Yu, J. Ding, P. Bryant, J. Huang, X. Tu, Plasma-enhanced catalytic synthesis of ammonia over a Ni/Al2O3 catalyst at near-room temperature: insights into the importance of the catalyst surface on the reaction mechanism, ACS Catal. 9 (12) (2019) 10780–10793.
[109] K.H. Rouwenhorst, H.-H. Kim, L. Lefferts, Vibrationally excited activation of N2 in plasma-enhanced catalytic ammonia synthesis: a kinetic analysis, ACS Sustain. Chem. Eng. 7 (20) (2019) 17515–17522.
[110] T. Mizushima, K. Matsumoto, H. Ohkita, N. Kakuta, Catalytic effects of metal-loaded membrane-like alumina tubes on ammonia synthesis in atmospheric pressure plasma by dielectric barrier discharge, Plasma Chem. Plasma Process. 27 (2007) 1–11.
[111] A. Gómez-Ramírez, J. Cotrino, R. Lambert, A. González-Elipe, Efficient synthesis of ammonia from N2 and H2 alone in a ferroelectric packed-bed DBD reactor, Plasma Sources Sci. Technol. 24 (6) (2015) 065011.
[112] A. Gómez-Ramírez, A.M. Montoro-Damas, J. Cotrino, R.M. Lambert, A.R. González-Elipe, About the enhancement of chemical yield during the atmospheric plasma synthesis of ammonia in a ferroelectric packed bed reactor, Plasma Process. Polym. 14 (6) (2017) 1600081.
[113] G. Akay, K. Zhang, Process intensification in ammonia synthesis using novel coassembled supported microporous catalysts promoted by nonthermal plasma, Ind. Eng. Chem. Res. 56 (2) (2017) 457–468.
[114] B.S. Patil, N. Cherkasov, N.V. Srinath, J. Lang, A.O. Ibhadon, Q. Wang, V. Hessel, The role of heterogeneous catalysts in the plasma-catalytic ammonia synthesis, Catal. Today 362 (2021) 2–10.
[115] Y. Ma, Y. Tian, Y. Zeng, X. Tu, Plasma synthesis of ammonia in a tangled wire dielectric barrier discharge reactor: effect of electrode materials, J. Eng. Inst. 99 (2021) 137–144.
[116] F. Gorky, H.M. Nguyen, J.M. Lucero, S. Guthrie, J.M. Crawford, M.A. Carreon, M.L. Carreon, CC3 porous organic cage crystals and membranes for the non-thermal plasma catalytic ammonia synthesis, Chem. Eng. J. Adv. 11 (2022) 100340.
[117] Z. Meng, J.-X. Yao, C.-N. Sun, X. Kang, R. Gao, H.-R. Li, B. Bi, Y.-F. Zhu, J.-M. Yan, Q. Jiang, Efficient ammonia production beginning from enhanced air activation, Adv. Energy Mater. 12 (38) (2022) 2202105.
[118] S. Li, Y. Shao, H. Chen, X. Fan, Nonthermal plasma catalytic ammonia synthesis over a Ni catalyst supported on MgO/SBA-15, Ind. Eng. Chem. Res. 61 (9) (2022) 3292–3302.
[119] E. Meloni, L. Cafiero, M. Martino, V. Palma, Structured catalysts for non-thermal plasma-assisted ammonia synthesis, Energies 16 (7) (2023) 3218.
[120] L. Hollevoet, F. Jardali, Y. Gorbanev, J. Creel, A. Bogaerts, J.A. Martens, Towards green ammonia synthesis through plasma-driven nitrogen oxidation and catalytic reduction, Angew. Chem. 132 (52) (2020) 24033–24037.
[121] B. Zhang, J. Li, H. Zuo, K. Kamiya, Y. Chen, G. Chen, N. Kobayashi, B. Wu, Reinforcement of fluidized catalysts with DBD plasma assisted for green ammonia synthesis, Int. J. Hydrog. Energy 67 (2024) 521–531.
[122] Y. Jing, F. Gong, S. Wang, W. Wang, P. Yang, E. Fu, R. Xiao, Activating the synergistic effect in Ni-co bimetallic MOF for enhanced plasma-assisted ammonia synthesis, Fuel 368 (2024) 131686.
[123] A. Bajpai, S. Kumar, Tailoring the surface acidity of catalyst to enhance nonthermal plasma-assisted ammonia synthesis rates, Mol. Catal. 557 (2024) 113961.
[124] A. Denra, S. Saud, D.B. Nguyen, Q.T. Trinh, T.-K. Nguyen, H. An, N.-T. Nguyen, S. Teke, Y.S. Mok, Nitrogen fixation by rotational gliding arc plasma at surrounding conditions, J. Clean. Prod. 436 (2024) 140618.
[125] Y. Wang, Q. Wang, S. Sun, Y. Xin, X. Zhu, B. Sun, Highly efficient ammonia synthesis by gas–liquid interface pulsed discharge plasma: A synthesis method without hydrogen, ACS Sustain. Chem. Eng. 11 (35) (2023) 13070–13080.
[126] H.M. Nguyen, F. Gorky, S. Guthrie, M.L. Carreon, Sustainable ammonia synthesis from nitrogen wet with sea water by single-step plasma catalysis, Catal. Today 418 (2023) 114141.
[127] K. Li, S. Chen, H. Wang, F. Wang, Plasma-assisted ammonia synthesis over Ni/LaOF: Dual active centers consisting of oxygen vacancies and Ni, Appl. Catal. A Gener. 650 (2023) 118983.
[128] T. Haruyama, T. Namise, N. Shimoshimizu, S. Uemura, Y. Takatsuji, M. Hino, R. Yamasaki, T. Kamachi, M. Kohno, Non-catalyzed one-step synthesis of ammonia from atmospheric air and water, Green Chem. 18 (16) (2016) 4536–4541.
[129] T. Sakakura, S. Uemura, M. Hino, S. Kiyomatsu, Y. Takatsuji, R. Yamasaki, M. Morimoto, T. Haruyama, Excitation of H2O at the plasma/water interface by UV irradiation for the elevation of ammonia production, Green Chem. 20 (3) (2018) 627–633.
[130] R. Hawtof, S. Ghosh, E. Guarr, C. Xu, R. Mohan Sankaran, J.N. Renner, Catalyst-free, highly selective synthesis of ammonia from nitrogen and water by a plasma electrolytic system, Sci. Adv. 5 (1) (2019) eaat5778.
[131] Y. Kubota, K. Koga, M. Ohno, T. Hara, Synthesis of ammonia through direct chemical reactions between an atmospheric nitrogen plasma jet and a liquid, Plasma Fusion Res. 5 (2010) 042–042.
[132] P. Peng, P. Chen, M. Addy, Y. Cheng, Y. Zhang, E. Anderson, N. Zhou, C. Schiappacasse, R. Hatzenbeller, L. Fan, et al., In situ plasma-assisted atmospheric nitrogen fixation using water and spray-type jet plasma, Chem. Commun. 54 (23) (2018) 2886–2889.
[133] T. Sakakura, N. Murakami, Y. Takatsuji, M. Morimoto, T. Haruyama, Contribution of discharge excited atomic N, N2*, and N2+ to a plasma/liquid interfacial reaction as suggested by quantitative analysis, ChemPhysChem 20 (11) (2019) 1467–1474.
[134] H. Gao, G. Wang, Z. Huang, L. Nie, D. Liu, X. Lu, G. He, K.K. Ostrikov, Plasma-activated mist: Continuous-flow, scalable nitrogen fixation, and aeroponics, ACS Sustain. Chem. Eng. 11 (11) (2023) 4420–4429.
[135] D. Ye, S.C.E. Tsang, Prospects and challenges of green ammonia synthesis, Nat. Synth. 2 (7) (2023) 612–623.
[136] F. Ma, L. Guo, Z. Li, X. Zeng, Z. Zheng, W. Li, F. Zhao, W. Yu, A review of current advances in ammonia combustion from the fundamentals to applications in internal combustion engines, Energies 16 (17) (2023) 6304.
[137] A.J. Medford, A. Vojvodic, J.S. Hummelshøj, J. Voss, F. Abild-Pedersen, F. Studt, T. Bligaard, A. Nilsson, J.K. Nørskov, From the sabatier principle to a predictive theory of transition-metal heterogeneous catalysis, J. Catal. 328 (2015) 36–42.
[138] L. Grajciar, C.J. Heard, A.A. Bondarenko, M.V. Polynski, J. Meeprasert, E.A. Pidko, P. Nachtigall, Towards operando computational modeling in heterogeneous catalysis, Chem. Soc. Rev. 47 (22) (2018) 8307–8348.
[139] Y. Wang, W. Yang, S. Xu, S. Zhao, G. Chen, A. Weidenkaff, C. Hardacre, X. Fan, J. Huang, X. Tu, Shielding protection by mesoporous catalysts for improving plasma-catalytic ambient ammonia synthesis, J. Am. Chem. Soc. 144 (27) (2022) 12020–12031.
[140] J. Mu, X.-W. Gao, T. Yu, L.-K. Zhao, W.-B. Luo, H. Yang, Z.-M. Liu, Z. Sun, Q.-F. Gu, F. Li, Ambient electrochemical ammonia synthesis: From theoretical guidance to catalyst design, Adv. Sci. (2024) 2308979.
[141] M.B. Yaala, A. Saeedi, D.-F. Scherrer, L. Moser, R. Steiner, M. Zutter, M. Oberkofler, G. De Temmerman, L. Marot, E. Meyer, Plasma-assisted catalytic formation of ammonia in N 2–H 2 plasma on a tungsten surface, Phys. Chem. Chem. Phys. 21 (30) (2019) 16623–16633.
[142] S. Zen, N. Takeuchi, Y. Teramoto, Ammonia synthesis using atmospheric pressure fluidized bed plasma, J. Phys. D: Appl. Phys. 57 (11) (2023) 115203.
[143] A. Bogaerts, X. Tu, J.C. Whitehead, G. Centi, L. Lefferts, O. Guaitella, F. Azzolina-Jury, H.-H. Kim, A.B. Murphy, W.F. Schneider, et al., The 2020 plasma catalysis roadmap, J. Phys. D: Appl. Phys. 53 (44) (2020) 443001.
[144] G. Xu, C. Cai, T. Wang, Toward sabatier optimal for ammonia synthesis with paramagnetic phase of ferromagnetic transition metal catalysts, J. Am. Chem. Soc. 144 (50) (2022) 23089–23095.

[145] C.J. Jacobsen, S. Dahl, B.S. Clausen, S. Bahn, A. Logadottir, J.K. Nørskov, Catalyst design by interpolation in the periodic table: bimetallic ammonia synthesis catalysts, J. Am. Chem. Soc. 123 (34) (2001) 8404–8405.
[146] P. Mehta, P. Barboun, F.A. Herrera, J. Kim, P. Rumbach, D.B. Go, J.C. Hicks, W.F. Schneider, Overcoming ammonia synthesis scaling relations with plasma-enabled catalysis, Nat. Catal. 1 (4) (2018) 269–275.
[147] H.-H. Kim, A.A. Abdelaziz, Y. Teramoto, T. Nozaki, K. Hensel, Y.-S. Mok, S. Saud, D.B. Nguyen, D.H. Lee, W.S. Kang, Interim report of plasma catalysis: footprints in the past and blueprints for the future, Int. J. Plasma Environ. Sci. Technol. 15 (1) (2021) e01004.
[148] H.-H. Kim, Y. Teramoto, N. Negishi, A. Ogata, A multidisciplinary approach to understand the interactions of nonthermal plasma and catalyst: A review, Catal. Today 256 (2015) 13–22.
[149] Y. Engelmann, K. van't Veer, Y. Gorbanev, E.C. Neyts, W.F. Schneider, A. Bogaerts, Plasma catalysis for ammonia synthesis: a microkinetic modeling study on the contributions of Eley–Rideal reactions, ACS Sustain. Chem. Eng. 9 (39) (2021) 13151–13163.
[150] C. Sellers, T.P. Senftle, Ammonia synthesis takes NO for an answer, Nat. Energy 8 (11) (2023) 1184–1185.
[151] Y. Ren, C. Yu, L. Wang, X. Tan, Z. Wang, Q. Wei, Y. Zhang, J. Qiu, Microscopic-level insights into the mechanism of enhanced NH3 synthesis in plasma-enabled cascade N2 oxidation–electroreduction system, J. Am. Chem. Soc. 144 (23) (2022) 10193–10200.
[152] Z. Liu, Y. Tian, G. Niu, X. Wang, Y. Duan, Direct oxidative nitrogen fixation from air and H2O by a water falling film dielectric barrier discharge reactor at ambient pressure and temperature, ChemSusChem 14 (6) (2021) 1507–1511.
[153] Y. Wang, A. Xu, Z. Wang, L. Huang, J. Li, F. Li, J. Wicks, M. Luo, D.-H. Nam, C.-S. Tan, et al., Enhanced nitrate-to-ammonia activity on copper–nickel alloys via tuning of intermediate adsorption, J. Am. Chem. Soc. 142 (12) (2020) 5702–5708.
[154] J. Liang, Z. Li, L. Zhang, X. He, Y. Luo, D. Zheng, Y. Wang, T. Li, H. Yan, B. Ying, et al., Advances in ammonia electrosynthesis from ambient nitrate/nitrite reduction, Chem (2023).
[155] J. Sun, R. Zhou, J. Hong, Y. Gao, Z. Qu, Z. Liu, D. Liu, T. Zhang, R. Zhou, K.K. Ostrikov, et al., Sustainable ammonia production via nanosecond-pulsed plasma oxidation and electrocatalytic reduction, Appl. Catal. B 342 (2024) 123426.
[156] W.P. Liang, X.-M. Zhang, P.-W. Bai, Z. Zhang, J.-H. Chen, W. Liu, Z.-H. Sun, Y. Feng, G. Yang, H.-M. Tong, et al., Cascade N2 reduction process with DBD plasma oxidation and electrocatalytic reduction for continuous ammonia synthesis, Environ. Sci. Technol. 57 (39) (2023) 14558–14568.
[157] R. Carapellucci, L. Giordano, Steam, dry and autothermal methane reforming for hydrogen production: A thermodynamic equilibrium analysis, J. Power Sources 469 (2020) 228391.
[158] X. Wang, Q. Huang, S. Ding, W. Liu, J. Mei, J. Luo, L. Lei, F. He, et al., Micro hollow cathode excited dielectric barrier discharge (DBD) plasma bubble and the application in organic wastewater treatment, Sep. Purif. Technol. 240 (2020) 116659.
[159] T. Zhang, R. Zhou, P. Wang, A. Mai-Prochnow, R. McConchie, W. Li, R. Zhou, E.W. Thompson, K.K. Ostrikov, P.J. Cullen, Degradation of cefixime antibiotic in water by atmospheric plasma bubbles: Performance, degradation pathways and toxicity evaluation, Chem. Eng. J. 421 (2021) 127730.
[160] Y. Liu, H. Zhang, J. Sun, J. Liu, X. Shen, J. Zhan, A. Zhang, S. Ognier, S. Cavadias, P. Li, Degradation of aniline in aqueous solution using non-thermal plasma generated in microbubbles, Chem. Eng. J. 345 (2018) 679–687.
[161] X. Zhang, D. Lohse, Perspectives on surface nanobubbles, Biomicrofluidics 8 (4) (2014).
[162] X. Li, B. Peng, Q. Liu, J. Liu, L. Shang, Micro and nanobubbles technologies as a new horizon for CO2-EOR and CO2 geological storage techniques: A review, Fuel 341 (2023) 127661.
[163] N. Guan, Y. Wang, B. Wen, X. Wang, J. Hu, L. Zhang, The regulation of surface nanobubble generation via solvent exchange on different substrates, Colloids Surf. A 676 (2023) 132290.
[164] D. Lohse, X. Zhang, et al., Surface nanobubbles and nanodroplets, Rev. Modern Phys. 87 (3) (2015) 981.
[165] Y. Gao, A.M. Dashliborun, J.Z. Zhou, X. Zhang, Formation and stability of cavitation microbubbles in process water from the oilsands industry, Ind. Eng. Chem. Res. 60 (7) (2021) 3198–3209.
[166] N. Rao, X. Chu, K. Hadinoto, R. Zhou, T. Zhang, B. Soltani, C. Bailey, F.J. Trujillo, G. Leslie, S. Prescott, et al., Algal cell inactivation and damage via cold plasma-activated bubbles: Mechanistic insights and process benefits, Chem. Eng. J. 454 (2023) 140304.
[167] K. Papalexopoulou, X. Huang, A. Ronen, C.A. Aggelopoulos, Reactive species and mechanisms of perfluorooctanoic acid (PFOA) degradation in water by cold plasma: The role of HV waveform, reactor design, water matrix and plasma gas, Sep. Purif. Technol. (2024) 126955.
[168] A. Patange, P. Lu, D. Boehm, P. Cullen, P. Bourke, Efficacy of cold plasma functionalised water for improving microbiological safety of fresh produce and wash water recycling, Food Microbiol. 84 (2019) 103226.
[169] R. Zhou, R. Zhou, P. Wang, B. Luan, X. Zhang, Z. Fang, Y. Xian, X. Lu, K.K. Ostrikov, K. Bazaka, Microplasma bubbles: reactive vehicles for biofilm dispersal, ACS Appl. Mater. Interfaces 11 (23) (2019) 20660–20669.
[170] K. Tachibana, T. Nakamura, Comparative study of discharge schemes for production rates and ratios of reactive oxygen and nitrogen species in plasma activated water, J. Phys. D: Appl. Phys. 52 (38) (2019) 385202.
[171] M.-C. Wu, S. Uehara, J.-S. Wu, Y. Xiao, T. Nakajima, T. Sato, Dissolution enhancement of reactive chemical species by plasma-activated microbubbles jet in water, J. Phys. D: Appl. Phys. 53 (48) (2020) 485201.
[172] H. Zhang, P. Li, A. Zhang, Z. Sun, J. Liu, P. Héroux, Y. Liu, Enhancing interface reactions by introducing microbubbles into a plasma treatment process for efficient decomposition of PFOA, Environ. Sci. Technol. 55 (23) (2021) 16067–16077.
[173] Y. Liu, Q. Wang, C. Wang, A. Zhang, K. Huang, J. Liu, A.C. Miruka, Q. Han, Y. Guo, Degradation of dichloroacetic acid in a novel corona discharge reactor integrated with microbubbles generation, Sep. Purif. Technol. 274 (2021) 119019.
[174] Z. Saedi, M. Kuddushi, Y. Gao, D. Panchal, B. Zeng, S.E. Pour, H. Shi, X. Zhang, Stable and efficient microbubble-enhanced cold plasma activation for treatment of flowing water, Sustain. Mater. Technol. (2024) e00887.
[175] Y. Gao, M. Li, C. Sun, X. Zhang, Microbubble-enhanced water activation by cold plasma, Chem. Eng. J. 446 (2022) 137318.
[176] A. Filipić, D. Dobnik, I. Gutiérrez-Aguirre, M. Ravnikar, T. Košir, Š. Baebler, A. Štern, B. Žegura, M. Petkovšek, M. Dular, et al., Cold plasma within a stable supercavitation bubble–A breakthrough technology for efficient inactivation of viruses in water, Environ. Int. 182 (2023) 108285.
[177] Q. Wu, H. Luo, H. Wang, Z. Liu, L. Zhang, Y. Li, X. Zou, X. Wang, Simultaneous hydrodynamic cavitation and nanosecond pulse discharge plasma enhanced by oxygen injection, Ultrason. Sonochem. 99 (2023) 106552.
[178] Y. Gao, Z. Saedi, H. Shi, B. Zeng, B. Zhang, X. Zhang, Machine learning-assisted optimization of microbubble-enhanced cold plasma activation for water treatment, ACS ES&T Water (2024).
[179] P. Peng, C. Schiappacasse, N. Zhou, M. Addy, Y. Cheng, Y. Zhang, E. Anderson, D. Chen, Y. Wang, Y. Liu, et al., Plasma in situ gas–liquid nitrogen fixation using concentrated high-intensity electric field, J. Phys. D: Appl. Phys. 52 (49) (2019) 494001.
[180] Q. Wu, R. van de Krol, Selective photoreduction of nitric oxide to nitrogen by nanostructured TiO2 photocatalysts: role of oxygen vacancies and iron dopant, J. Am. Chem. Soc. 134 (22) (2012) 9369–9375.
[181] S. Chen, W. Feng, Q. Geng, F. Dong, H. Wang, Z. Wu, A new strategy for plasma-catalytic reduction of NO to N2 on the surface of modified Bi2MoO6, Chem. Eng. J. 440 (2022) 135754.
[182] Y. Liu, J.-W. Wang, J. Zhang, T.-T. Qi, G.-W. Chu, H.-K. Zou, B.-C. Sun, NOx removal by non-thermal plasma reduction: experimental and theoretical investigations, Front. Chem. Sci. Eng. 16 (10) (2022) 1476–1484.
[183] G.-F. Chen, Y. Yuan, H. Jiang, S.-Y. Ren, L.-X. Ding, L. Ma, T. Wu, J. Lu, H. Wang, Electrochemical reduction of nitrate to ammonia via direct eight-electron transfer using a copper–molecular solid catalyst, Nat. Energy 5 (8) (2020) 605–613.
[184] E. Pérez-Gallent, M.C. Figueiredo, I. Katsounaros, M.T. Koper, Electrocatalytic reduction of nitrate on copper single crystals in acidic and alkaline solutions., Electrochim. Acta 227 (2017) 77–84.
[185] W. Liu, M. Xia, C. Zhao, B. Chong, J. Chen, H. Li, H. Ou, G. Yang, Efficient ammonia synthesis from the air using tandem non-thermal plasma and electrocatalysis at ambient conditions, Nature Commun. 15 (1) (2024) 3524.
[186] P.H. van Langevelde, I. Katsounaros, M.T. Koper, Electrocatalytic nitrate reduction for sustainable ammonia production, Joule 5 (2) (2021) 290–294.
[187] Z. Deng, C. Ma, Z. Li, Y. Luo, L. Zhang, S. Sun, Q. Liu, J. Du, Q. Lu, B. Zheng, et al., High-efficiency electrochemical nitrate reduction to ammonia on a Co3O4 nanoarray catalyst with cobalt vacancies, ACS Appl. Mater. Interfaces 14 (41) (2022) 46595–46602.
[188] H. Xu, Y. Ma, J. Chen, W.-x. Zhang, J. Yang, Electrocatalytic reduction of nitrate–a step towards a sustainable nitrogen cycle, Chem. Soc. Rev. 51 (7) (2022) 2710–2758.
[189] W. Li, S. Zhang, J. Ding, J. Liu, Z. Wang, H. Zhang, J. Ding, L. Chen, C. Liang, Sustainable nitrogen fixation to produce ammonia by electroreduction of plasma-generated nitrite, ACS Sustain. Chem. Eng. 11 (3) (2023) 1168–1177.
[190] S. Chen, S. Perathoner, C. Ampelli, C. Mebrahtu, D. Su, G. Centi, Room-temperature electrocatalytic synthesis of NH3 from H2O and N2 in a gas–liquid–solid three-phase reactor, ACS Sustain. Chem. Eng. 5 (8) (2017) 7393–7400.
[191] Y. Ren, C. Yu, X. Tan, H. Huang, Q. Wei, J. Qiu, Strategies to suppress hydrogen evolution for highly selective electrocatalytic nitrogen reduction: challenges and perspectives, Energy Environ. Sci. 14 (3) (2021) 1176–1193.
[192] Y. Wang, W. Zhou, R. Jia, Y. Yu, B. Zhang, Unveiling the activity origin of a copper-based electrocatalyst for selective nitrate reduction to ammonia, Angew. Chem. Int. Ed. 59 (13) (2020) 5350–5354.
[193] Y. Liu, C.-W. Wang, X.-F. Xu, B.-W. Liu, G.-M. Zhang, Z.-W. Liu, Q. Chen, H.-B. Zhang, Synergistic effect of Co–Ni bimetal on plasma catalytic ammonia synthesis, Plasma Chem. Plasma Process. 42 (2) (2022) 267–282.
[194] T. Zhu, Q. Chen, P. Liao, W. Duan, S. Liang, Z. Yan, C. Feng, Single-atom Cu catalysts for enhanced electrocatalytic nitrate reduction with significant alleviation of nitrite production, Small 16 (49) (2020) 2004526.

[195] J. John, D.R. MacFarlane, A.N. Simonov, The why and how of NO x electroreduction to ammonia, Nat. Catal. 6 (12) (2023) 1125–1130.
[196] Y. Huan, Y. Jiang, L. Li, Y. He, Q. Cheng, Y. Cao, M. Wang, C. Yan, T. Qian, Recent advances in electrocatalysts for sustainable electrosynthesis of ammonia and urea from ambient nitrite reduction and C–N coupling, ACS Mater. Lett. 5 (12) (2023) 3347–3363.
[197] S.-L. Meng, C. Zhang, C. Ye, J.-H. Li, S. Zhou, L. Zhu, X.-B. Li, C.-H. Tung, L.-Z. Wu, Cobaloximes: selective nitrite reduction catalysts for tandem ammonia synthesis, Energy Environ. Sci. 16 (4) (2023) 1590–1596.
[198] I. Muzammil, Y.-N. Kim, H. Kang, D.K. Dinh, S. Choi, C. Jung, Y.-H. Song, E. Kim, J.M. Kim, D.H. Lee, Plasma catalyst-integrated system for ammonia production from H2O and N2 at atmospheric pressure, ACS Energy Lett. 6 (8) (2021) 3004–3010.
[199] PlasmaLeap, URL https://www.plasmaleap.com/efuels-chemicals.
[200] VitalFluid, URL https://vitalfluid.com/products/.
[201] H.-H. Kim, Y. Teramoto, A. Ogata, H. Takagi, T. Nanba, Atmospheric-pressure nonthermal plasma synthesis of ammonia over ruthenium catalysts, Plasma Process. Polym. 14 (6) (2017) 1600157.
[202] L. Wang, M. Xia, H. Wang, K. Huang, C. Qian, C.T. Maravelias, G.A. Ozin, Greening ammonia toward the solar ammonia refinery, Joule 2 (6) (2018) 1055–1074.
[203] L. Hollevoet, E. Vervloessem, Y. Gorbanev, A. Nikiforov, N. De Geyter, A. Bogaerts, J.A. Martens, Energy-efficient small-scale ammonia synthesis process with plasma-enabled nitrogen oxidation and catalytic reduction of adsorbed NOx, ChemSusChem 15 (10) (2022) e202102526.
[204] O.A. Ojelade, S.F. Zaman, B.-J. Ni, Green ammonia production technologies: A review of practical progress, J. Environ. Manag. 342 (2023) 118348.
[205] C. Smith, A.K. Hill, L. Torrente-Murciano, Current and future role of haber–bosch ammonia in a carbon-free energy landscape, Energy Environ. Sci. 13 (2) (2020) 331–344.
[206] J.G. Chen, R.M. Crooks, L.C. Seefeldt, K.L. Bren, R.M. Bullock, M.Y. Darensbourg, P.L. Holland, B. Hoffman, M.J. Janik, A.K. Jones, et al., Beyond fossil fuel–driven nitrogen transformations, Science 360 (6391) (2018) eaar6611.
[207] Z. Ke, D. He, X. Yan, W. Hu, N. Williams, H. Kang, X. Pan, J. Huang, J. Gu, X. Xiao, Selective NO x–electroreduction to ammonia on isolated ru sites, ACS Nano 17 (4) (2023) 3483–3491.
[208] J. Shao, H. Jing, P. Wei, X. Fu, L. Pang, Y. Song, K. Ye, M. Li, L. Jiang, J. Ma, et al., Electrochemical synthesis of ammonia from nitric oxide using a copper–tin alloy catalyst, Nat. Energy 8 (11) (2023) 1273–1283.
[209] H. Ma, R.K. Sharma, S. Welzel, M.C. van de Sanden, M.N. Tsampas, W.F. Schneider, Observation and rationalization of nitrogen oxidation enabled only by coupled plasma and catalyst, Nature Commun. 13 (1) (2022) 402.
[210] Y. Gao, K. Francis, X. Zhang, Review on formation of cold plasma activated water (PAW) and the applications in food and agriculture, Food Res. Int. 157 (2022) 111246.